COAL FIRE RESEARCH
A SINO-GERMAN INITIATIVE

Innovative Technologies for Exploration, Extinction and Monitoring of Coal Fires in North China

Final Report on
Gas and Temperature Measurements at
Fire Zones 3.2 & 8

WP 3410 Sampling along Regular Grids
WP 3420 In situ measurements (surface & bore holes)
WP 3430 Permanent Gas Monitoring

Prepared by: Dr. Stefan Schloemer

Date: 5. July 2006

Federal Institute for Geosciences and Natural Resources (BGR),
D - 30655 Hannover (Germany)

Executive Summary

This study was performed within the framework of the “Sino-German Coal Fire Research Initiative”. Since 2003 an extensive joint research program investigates natural coal fires in China. In Wuda, Inner Mongolia Autonomous Region (PRC), an area of 280.000 m² is affected by subsurface coal fires which can be related to small scale mining operations.

Analysis of combustion gases of two fire zones measured in 2004, clearly revealed, that a variety of combustion processes can be recognized. The occurrence of methane and carbon monoxide can be linked to coal pyrolysis (i.e. the chemical decomposition of organic materials by heating in the absence of oxygen or any other reagents) and molecular hydrogen results from coking, i.e. the generation of volatile constituents (water and coal-gas) or coal gasification processes (conversion of carbonaceous material into CO and H_2). No clear relationship between gas composition and temperature of the vent gases could be established. However, it could be shown that, besides the large emanations occurring through fractures significant amount of combustion gases can migrate through the overlying bedrock and/or superficial covering of fire zones.

For the first time combustion gases and temperatures of in-situ coal fires have been measured continuously over 5.5 months. At different sites close to the main combustion zone (~25m) of fire zone 8, one of the largest fire zones in this area, temperatures (three vents) and gas composition (one vent) were measured from June to October 2005 and complemented by the recording of meteorological data (wind direction & velocity, barometric pressure & ambient temperature). Temperature measurements in the gas emanating vents showed intense fluctuations (up to ±100°C within 48h) which could not be directly related to meteorological conditions. These short-term fluctuations were superimposed by long-term temperature trends which ranged from +100°C/month to -30°C/month. These variations are a result of the proceeding fire front. These findings are further confirmed by the change in gas composition. Over the measuring period the CO/CO_2 ratio significantly decreased. At the same time the temperature of the sampled vent increased by 35°C (80°C -> 115°C). Both findings indicate the approach of the main combustion zone. However, the observed trends are smaller than expected and indicate a very slow progress of the coal fire (< 10m/year).

During October 2005 water-flooding experiments were performed by the project partner DMT. Up to 15m³ of water were introduced at three different locations and the response on temperature and gas composition was measured by our group (Federal Institute for Geosciences and Natural Resources, BGR). During one experiment close to the gas measuring site (about 4.5m³ of water were injected) a significant change in gas composition was observed. Due to the limited subsequent monitoring period this change can only be attributed to a dilution with the evolving steam. A direct effect on the coal combustion processes cannot be revealed. Another experiment, where 15m³ of water were added close to the main coal combustion zone, lead to an intense steam production and a temperature drop from 290°C to 260°C in the nearby fracture was monitored in a short period. Temperature continued to decrease almost linearly for several days. This suggests that the flooding water had significantly influenced the combustion process and the temperature decline is a result of the subsequently cooling bed rock.

Table of Contents

Figures and Tables

1. Introduction

Outcropping coal seams and waste piles are burning around the world and lead to severe environmental and economic problems (Stracher & Taylor 2004). Besides the economic damages due to a reduction of the coal reserves, they cause land subsidence and affect the human health in nearby areas. Enormous quantities of noxious gases (SO_2, NO, CO_2, CO, CH_4) and particulate matter (ash) can be emitted into the atmosphere, condensation products can lead to water and soil pollution (Stracher & Taylor 2004; Stracher 2004, 2003, 1995).

Since 2003 a geo-scientific "Sino-German Coal Fire Research Initiative" investigates the coal fire problem in China. This project includes various partners from different geo-scientific fields and focuses on developing innovative technologies for exploration, extinction and monitoring of coal fires in China. As a prerequisite for the extinction of coal fires, the first phase of the project gave special attention to the processes which lead to coal fires (i.e. spontaneous combustion) and control their spatial and temporal development. One major aim of the "Sino-German Coal Fire Research Project" is to build static and, with time related information, dynamic 3-D models of the combustion processes. Many of the spontaneous combustion/hot coal fires were detected long after the fires had started due to lack of continuous and early combustion gas/smoke detection systems (De Rosa 2004). Detailed gas measurements (static and continuous) allow the indication of underground combustion processes and their temporal changes. Data obtained are an important basis for emission monitoring, dynamic modeling of coal fires and surveillance of potentially hazardous areas.

In-situ one-time gas and temperature measurements have been performed by different working groups (Federal Institute for Geosciences and Resources (BGR), Deutsche Montan Technologie GmbH) in 2004. The qualitative and quantitative in-situ measurements of combustion gases supported the identification of fire zones and provided indicators for the prevailing combustion process (see below) and resulted in a classification and mapping of the spatial distribution of cracks and vents as well as an estimation of the total gas flows (Litschke et al., submitted). However, from the review of the sparse gas-geochemical data on underground coal fires and our experience we knew that subsurface coal fires are very dynamic systems in time & space. Therefore it was important to carry out a long-term measurement of gas emanations.

Traditional gas-geochemical sampling requires that samples are taken directly from gas emanating vents or soil. This could be dangerous and can only be carried out on a weekly or even monthly basis for remote locations. A permanent continuous monitoring based on optical and/or chemical sensing techniques coupled with temperature measurements is a superior option. Permanent multi-parameter measuring stations offers a wide range of potential applications and have been used by BGR for several years in the field of volcano and mud volcano monitoring (Faber et al. 2003; Seidl et al. 2003; Teschner et al. 2005, 2006; Delisle et al. 2005), earthquake prediction (Bräuer et. al., (submitted)), and CO_2 storage issues (Brune et al. 2003).

BGR built and operated a continuous monitoring of gas emanations over 5 months resulting in a high data density of combustion gas composition, vent temperatures and weather condition factors (i.e. barometric pressure, temperature, wind direction and

velocity) at a selected fire zone (FZ) in Wuda, Inner Mongolia Autonomous Region, PRC.

2. Combustion Gases of Natural Coal Fires

Gases deriving from coal conversion under high temperatures (e.g. coke production, coal gasification) are a result of different processes: drying, devolatilization, gasification and combustion (e.g. Stillman 1979; Dikeç et al. 1994). Although most of the scientific results derive from the industrial gasification research, they can explain the gases emanating from natural coal fires. Other potential industrial processes based on coal conversion, e.g. liquefaction of coal to liquids and tars or direct conversion of coal (e.g. Schobert & Song 2002), are beyond the scope of this paper and will not be discussed.

2.1. Drying

During the first step of coal conversion the moist coal releases the adsorbed water by evaporation. Pre-existing adsorbed gases like methane and CO_2 - originating from the pyrolysis process due to the initial burying - are desorbed because the adsorption capacity is drastically reduced due to the coal fire induced temperature increase (Busch et al. 2003; Krooss et al. 2002).

2.2. Devolatilization (Pyrolysis)

Devolatilization (or pyrolysis) is formally defined as chemical decomposition of organic materials by heating in the absence of oxygen under hydrous or dry conditions. During this process methane and higher homologues, aromatic hydrocarbons, CO_2, CO, H_2, H_2S and SO_2, N_2 and significant amounts of water are generated. The intensity of this process is highly temperature dependant and the formation of the volatile components depends also strongly on coal type and maturity (Feng et al. 2004) and composition.

Pyrolysis implies disproportion reactions from the organic molecules during the different stages of coal maturation. During the first stage (“peat formation”) only mechanical compaction and water elimination take place. In the second stage (“catagenesis”) two reactions occur: release of water (retaining the carbon chain length) by dehydration processes, decarboxylation reactions (release of CO_2) and phenol condensations. During late catagenesis (i.e. the C-content of the organic matter is > 80%) the following reactions in order of increasing maturity occur: dealkylation (release of C_nH_{2n+1} radicals), demethylation (methane release), and thermal cleavage of alkyl chains, thermal demethanation (methane release), aromatic condensation (H_2 release) and finally the graphitization (H_2 release). These are the general processes which lead to hydrocarbon generation from organic matter during natural burying of organic matter (Tissot & Welte 1984, Hunt 1996 and references herein) under geological heating rates and moderately temperatures (250°C). The final product of these reaction steps is anthracite.

Pyrolysis reactions occur also during industrial coal gasification when the temperature increases and the velocity of the gasification front is low (Kuyper et al. 1996). The tar and volatile yields depend strongly on the heating rate (e.g. Zhuo et al. 2003). Significant amounts of volatiles and tar in industrial coal gasifiers are generated at temperatures above 400°C (Gönenç Sunol & Sunol 1994).

2.3. Gasification

The gasification process is a reaction of char with carbon dioxide (CO_2) and steam to produce carbon monoxide (CO) and molecular hydrogen (H_2). Several industrial applied methods belong to this category of coal reaction processes: coke reduction, gasification in fluidized bed gasifiers, counter and co-current fixed bed gasifiers and entrained flow gasifiers (e.g. de Jong et al. 2003; Barysheva et al. 2003; Thunman & Leckner 2003; Wall et al. 2003) and underground coal gasification. They are principally identical being only different in process engineering design (pressure and temperature conditions, adding of H_2O/steam to enhance reaction).

2.3.1. Coking

In the process of converting coal into coke the volatile matter in the coal is vaporized and the remaining char reacts with the generated gas. Usually, carbon, either as coal, graphite or diamond does not react with water under normal conditions. Under more forcing conditions (i.e. high temperatures), the reaction becomes important. The endothermic *water-gas reaction*

$$C + H_2O \Rightarrow CO + H_2$$

generates the resulting „water gas“. An important secondary reaction is the *water-gas shift reaction*, whose effectiveness depends on the available C/H ratio (Thompson 1999):

$$CO + H_2O \Rightarrow CO_2 + H_2$$

A variety of secondary reactions, e.g. methanation reactions, can occur (Stillman 1979):

$$C + CO_2 \Rightarrow 2\ CO$$
$$CO_2 + H_2 \Rightarrow CO + H_2O$$
$$C + 2\ H_2 \Rightarrow CH_4$$
$$CO + 3\ H_2 \Rightarrow CH_4 + H_2O$$

The so-called coke-oven gas is driven off the process at very high temperatures (up to 1400°C). The typical composition of the gas (water saturated at 80°C) is 47 % H_2O, 29% H_2, 13% CH_4, 5% N_2, 3% CO and 1% higher hydrocarbons. Raw coke oven gas also contains various contaminants, which give it its unique characteristics (e.g. Li et al. 1999). These are made mainly of tar vapors, light oil vapors (aromatics, mainly benzene, toluene and xylene), naphthalene vapor and ammonia, hydrogen sulfide and hydrogen cyanide gas. In this industrial process, the coke oven gas is cleaned and recycled for further use. *Natural coke* is coal altered by locally elevated heat flows induced by intrusive bodies (Kwiecińska & Peterson 2004) and has been described for several years (Kwiecińska et al. 1992, 1995; Taylor et al. 1998).

2.3.2. Industrial Scale Gasification

The gasification process was originally developed in the 1800s to produce gas for domestic use (lighting, cooking) and street lighting (Schobert 1987). Natural gas and electricity substituted before long the town gas, but the gasification process has been utilized for the production of synthetic chemicals and fuels since the 1920s. 20% of

coal gasification plants are used for electrical power generation (Minchener 2005). The main difference between coke production and industrial coal gasification is the adding of water/steam (blown through the hot coke) to increase the reaction yield of the water-gas and water-gas shift reaction (e.g. Onozaki et al. 2006), hence increasing the yield of the favored component H_2. The product gas (producer gas, water gas, town gas, synthetic natural gas) varies in composition, depending on the reactant gas in the process (air & steam or oxygen & steam), temperature and pressure conditions (e.g. Ünal et. al 1994; Megaritis et al. 1998), the coal type and molar O/C ratio of the feed (Harris et al. 2006). In the low-temperature part of the reactor the abovementioned reactions occur (typically in the temperature range of 220-550°C), but the rate-limiting reaction is the gasification step of the char (Sekine et al. 2006).

Gasification reactors as mentioned above are operated at high temperatures, in particular in the combustion zone, where the partly degassed down moving coke is oxidized (combusted) to release heat and carbon dioxide. Oxygen blown gasifiers may reach temperatures of more than 1500°C (Megaritis 1998), but can operate at temperatures much lower (920°C, Ünal et al. 1994). The main reduction and gasification processes occur at temperatures typically between 600°C and 920°C (Ünal et al. 1998). These temperatures can easily be reached by natural underground coal fires. Temperatures in excess of > 800°C have been reported by Prakash & Gupta (1999) for coal fires in India, temperatures in excess of 1000°C have been described for Pleistocene coal fires (Zhang & Kroonenberg 1996; Kroonenberg & Zhang 1997). The existence of a partly melted rock in the hanging wall of coal fires (clinker, paralava) indicates temperatures of > 1300°C (Cosca et al. 1989; Heffern & Coats 2004). Although the extent and velocity of the reactions in industrial applications are much higher due to the operating conditions (i.e. elevated pressures) than in natural coal fires the same gas components can be expected.

2.3.3. Underground Coal Gasification

Underground coal gasification can best be described as an in situ controlled combustion of coal, producing combustible and economically valuable gases (e.g. Ökten & Didari 1994). At least two wells are drilled, one serving as supply well for the air/oxygen and steam inlet (injection well), the second one as exhaust for the produced gases (production well). A critical factor is the permeability linkage between the two wells across the coal bed which must be enhanced by additional measures, e.g. hydraulic fracturing, pneumatic linkage, explosive fracturing or electrolinking (Ökten & Didari 1994). The same reactions as described earlier occur in this process (Figure 1) and will also develop during a natural coal fire.

Gas composition of underground coal gasification has been described from various field experiments, for example of the “El Tremadal” pilot study in Spain (1993-1998). The dry gas composition of the gas outlet was around 40% CO_2, 9% CO 18% H_2, 8% CH_4, 8% H_2S and water (Creedy et al. 2001; Brasseur et al. 2002). Perkins (2004) published values for the Newman Spinney 5 field trial in Australia, where the dry gas composition was completely different (66.5% N_2, 0.8% CH_4, 9.4% H_2 15% CO_2 and 8% CO). Underground in-situ gasification of steep dipping coal seams led to 16% H_2 and 2.5% CH_4 in the final gas (Yang 2004). A pilot project of underground coal gasification (UCG) in the Liuzhuang Colliery, Tangshan, yielded an average of 40% H_2 (Yang et al. 2003). Jones & Thune (1982) measured up to 5% methane during a geochemical survey at the surface of an underground reactor in steeply dipping coal beds near Rawlins, Wyoming (USA).

A recent study has confirmed that ^{13}C isotopic abundance measurements for the system CO/CO_2 can be an indicator of the temperature inside in underground coal gasification unit (Brasseur et al. 2002). The enrichment in ^{13}C and D in the coaly organic matter remaining in the cuttings enabled Chandelle et al. (1993) to identify zones where combustion and gasification reactions had progressed furthest.

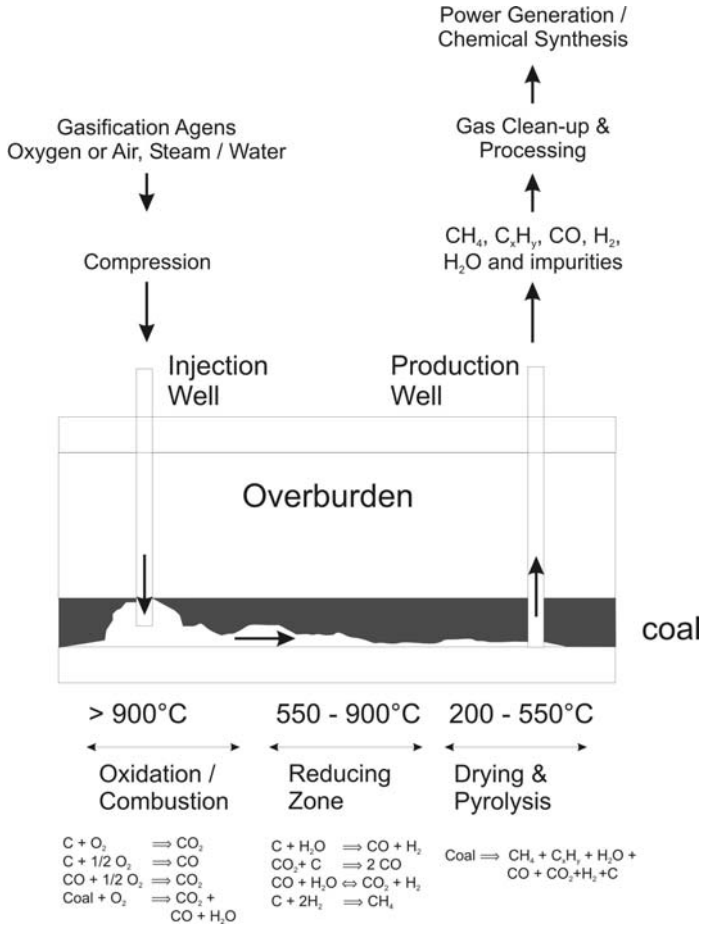

Figure 1: Principal sketch of underground coal gasification (modified after Ökten & Didari 1994)

2.4. Natural Coal Fires

As natural coal fires follow the same thermochemical principles like pyrolysis and gasification - in fact they are nothing different than an out-of-control underground gasification reactor – it is not surprising that the same gas components can be found in vents and cracks at the surface. Herman & McAteer (1999) measured combustion gases in boreholes close to the Loveridge Mine Fire (Fairmont, West Virginia) and found up to 18% CH_4 and 11500 ppm H_2. For an Illinois Mine Fire they reported up to 7% CO_2, 2.6% CH_4, 77.8% N_2, 0.93% Ar, 4343 ppm CO and 211 ppm H_2. Close to a mine fire at Somerset/Colorado (West Elk Mine) up to 2% CH_4 and 4600ppm H_2 were proven (U.S. Department of Labor, Mine Safety and Health Administration).

The Bureau of Mines (US Department of the Interior) has developed a diagnostic hydrocarbon index, to detect hot and cold subsurface zones by means of inter-

borehole communication test (Dalverny & Chaiken 1991; Kim 1986, 1991, 2004). This index, the molar fraction of higher hydrocarbons, will increase with temperature as heavier hydrocarbons are released from the coal (Mitchell 1996; Alvarez et al. 1997). However, the absolute value of the index does not depend on the temperature but on type and rank of the coal and it must be taken into account that methane and ethane/propane can also originate from liberated seam gas (coal bed methane). In addition other hydrocarbons like ethylene (C_2H_4), propylene (C_3H_6), acetylene (C_2H_2) have been used or proposed as mine fire indicator gases (Stracher & Taylor 2004; Herman & McAteer 1999) and as temperature indicator for the fire. Ethylene is released at lower temperatures (240°C) then propylene (300°C; Chamberlain 1971). Formaldehyde (CH_2O), formic acid (CH_2O_2), acetic acid ($C_2H_4O_2$) and glyoxal ($C_2H_2O_2$) have been suggested by Mitchell (1996) as diagnostic mine fire gases.

More often, CO and CO_2 are used as monitoring gas (Conti & Litton 1995; Edwards et al. 1999; De Rosa 2004) although there can be some interference with diesel combustion gases in coal mines. Different gas component ratios like the Jones-Trickett-Ratio[1] (Jones & Trickett 1955), the ratio of CO to CO_2 (Dalverny & Chaiken 1991), the air free CO concentration[2] and the Graham-Index[3] (Graham 1920) are used in active mines but have often yielded ambiguous results (Kim & Chaiken 1993; Kim 1986, 1991).

Hydrogen is mostly produced in a mine from battery charging, but is also one of the main gases which have been found in the air after an underground coal fire (afterdamp, Grosshandler 1995). Therefore hydrogen is seen as a good tracer for all smoldering processes and is recurrently used for early fire detection (Grosshandler 1995).

The above mentioned chemical reactions associated with “coal gasification” depend on the available water and high temperatures (which can easily be obtained in natural coal fires, see above). Consequently hydrogen generation is enhanced when water is used for coal fire extinguishing in the mine (see for example the Mine Rescue Manual of Saskatchewan Mine Emergency Response Program and the corresponding manual of the Pennsylvanian Bureau of Deep Mine Safety) or even on ship hazards where the fire fighting department passed on extinguishing the fire with water to avoid a secondary explosion due to the water gas reaction (e.g. Los Angeles Fire Department Historical Archive from September 9th 1981, fire on board of the M. S. Kartini). Another potential danger is the risk of steam explosions (Stracher & Tayler 2004).

2.5. Primary and Secondary Combustion

Generally speaking, the primary coal combustion process under oxidizing conditions yields carbon dioxide, carbon monoxide, unreacted oxygen (and nitrogen) as the main gases. In fact, the most efficient reaction possible generates only CO_2 and water vapor (complete combustion; Harju 1980). An important difference between coal combustion and coal gasification is the pollutant formation (Moreea-Taha 2000). The reducing atmosphere in gasification converts sulfur (S) from coal to hydrogen sulfide (H_2S) and

---

[1] Jones Tricket Ratio = $([CO_2]+0.75[CO] – 0.25[H_2])/(0.286[N_2] – [O_2])$

[2] $CO_{airfree} = ([CO]/(100 – 4.76[O_2])) * 100$

[3] Graham Index = $[CO]/(0.268[N_2] – [O_2]$ (with [CO] in ppm)

nitrogen (N) to ammonia (NH_3), whereas complete combustion (oxidation) produces sulfur dioxide (SO_2) and oxides of nitrogen (NO_x).

Secondary combustion in underground coal gasification and natural coal fires occurs if sufficient O_2 is available so that the generated combustible gas components (i.e. CO, H_2, CH_4) will be directly oxidized to CO_2 and H_2O. This reaction contributes to the overall calorific value of the coal and heat production of the underground gasification process. This secondary combustion of volatiles produced from the burning coal seam in the fracture or crack can markedly increase the convection of the gases (Huang et al. 2001).

3. Geological Setting of FZ 3.2 and FZ 8

The Wuda coalfield represents an isolated outcrop of Permo-Carboniferous strata in the northern part of the Helan Shan, a 300 km long range at the border between Ningxia and Inner Mongolia (Gielisch & Kahlen 2003) and is part of a North-South trending syncline with an extension of app. 10km in N-S direction and up to 5km in E-W direction (Gangopadhyay 2003). The syncline is confined to the West and North by the flat basin of the Gobi Desert, to the East lays the wide valley of the Huang He (Yellow River) and the Ordos massive.

Following the results of Diaz et al. (1983) and the IUGS 2000 report (following Jones 1995), the Permo-Carboniferous coal bearing strata belong to the Permian completely. This Permian sedimentary sequence (about 325 to 350 m total thickness) of the Wuda coalfield is made up by clastic sediments ranging from claystone to conglomeratic sandstones bearing 18 coal seams (numbering starting with the stratigraphically youngest formations). The sedimentary sequence, which is cut off in the centre of the structure (Gielisch & Kahlen 2003), belongs to the Lower Permian Yanghogou (C_{2y}) and Taiyuan (C_{3t}) formation, and Middle to Upper Permian Shanxi (P_1), and Shihexi (P_2) formations and demonstrate the typical cyclic sedimentation from coal to claystone to silt-/sandstone and back to claystone and coal. Typically, partly conglomeratic, coarse sandstones and occasional conglomerates between two coal seams were deposited during the sedimentary centre of a cycle.

The strata forming the lower part of the Upper Taiyuan Formation include the seams No. 18 to 9. At fire zone 8, the double seam 9 and 10 is underlain by a thick basal sandstone unit (16m) separated from seam 10 by a 3m thick mudstone sequence. Between seam 9 and 10 another mudstone interlayer with siderite concretions occurs. Seam 9 represents the boundary between the Lower Upper Taiyuan ($3_{t\ 2/1}$) and the Uppermost Taiyuan Formation ($3_{t\ 2/2}$). Seam 9 is overlain by 8m thick sequence of siltstones with plant debris and interrupted by thin sandstone interlayers. Above this sequence an alternated bedding of sandstones (partly including bed including drift wood and iron concretions) and mudstones occurs. The uppermost outcropping rock is made by sandstones (Gielisch & Kahlen 2003).

The study was conducted at fire zone 3.2 (FZ 3.2) and 8 (FZ 8) of the Wuda coal field located in the Inner Mongolia Autonomous Region.

FZ 3.2 is located in the north-west of the Wuda syncline at the outer rim of the structure. The strata shaping the smaller hills of BZ 3-2 belong to the oldest unit outcropping in the Wuda syncline (Gielisch & Kahlen 2003). The mixed layers of

sandstones, silt- to claystones and coal are part of the Lower Upper Taiyuan Formation and reach from the oldest seam, No. 15, to the seam No. 9 marking the boundary from the Upper Taiyuan Fm. to the Uppermost Taiyuan Fm. (Gielisch & Kahlen 2003). The stratigraphic sequence dips with angles from 5° up to 22° into a south-easterly direction. Most of the thermal activity in Fire Zone 3-2 takes place on a small pillar between two depressions caused by mining induced land subsidence. The gas emanating cracks or oriented in NW-SE directions (compare Figure 2).

FZ 8 is located in the western part of the Wuda syncline. It is one of the largest burning zones of the Wuda coalfield, where the seams No. 9 and No. 10 are burning intensely. The fire has caused massive landslides and up to 1 m wide cracks resulting in a massive collapsing of the overburden rock units (compare Figure 3). The strata are generally dipping into an easterly direction with angles between 10° and 20°. Due to the massive land slides within the whole area, these angles might be influenced by post fire events and may not represent the natural bedding conditions (Gielisch & Kahlen 2003).

4. Combustion Gases of Wuda Coal Fires (WP 3410 & WP 3420)

4.1. Field work 2004

Effective field work lasted from June 23rd to July 8th, 2004 (13 days) during the joint summer field campaign. Seven days were spent at fire zone 3.2, 6 measuring days at fire 8 (northern part). Due to the lack of time and the unfavorable surface conditions (FZ not accessible), no measurements were performed at the third test area fire 11. In total, including replicate measurements, 41 emission chamber & 63 compositional measurements at fire zone 3.2 and 3 emission chamber & 158 compositional measurements at fire zone 8 were carried out (Figure 2 and Figure 3). No measurements were performed at the study sites in Rujigou fire zone because the steep topography and the inhomogeneous ventilation zones do not allow for reliable gas/emission measurements in that area.

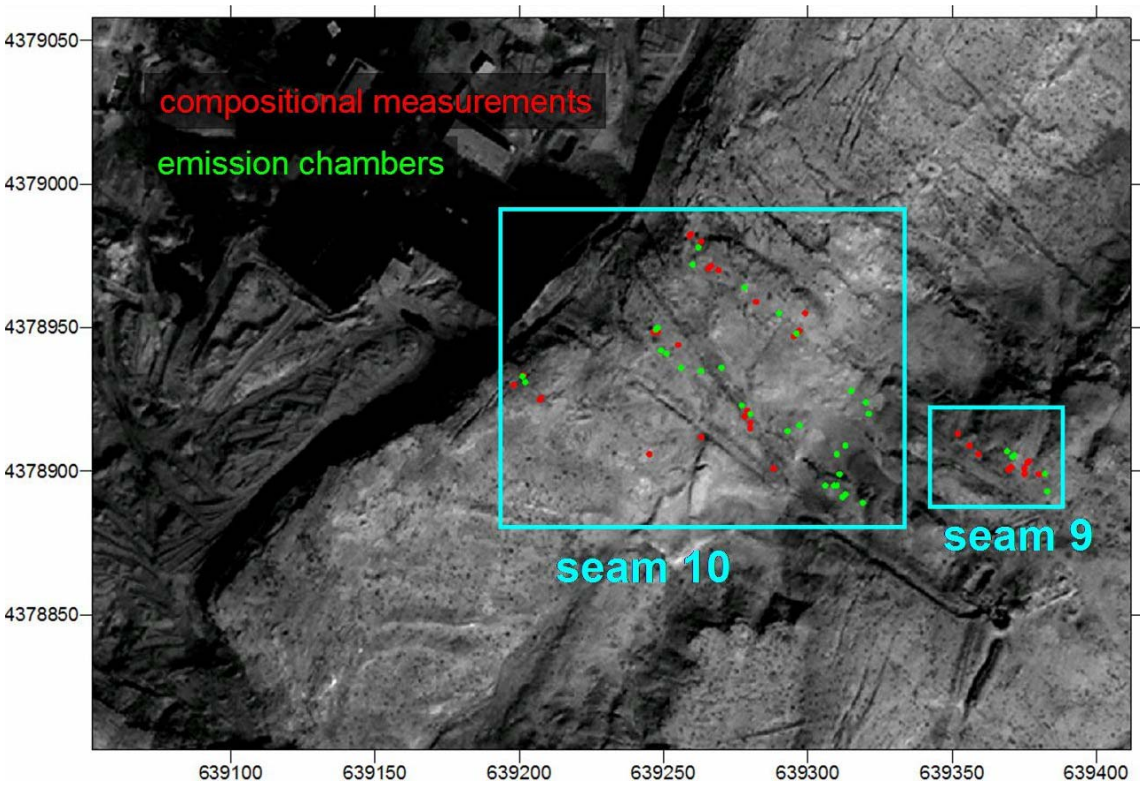

Figure 2: Sample locations at fire zone 3.2. Boxes indicate the locations of gas measurements related to the different burning seams 9 and 10. (compositional measurements in red, emission chamber measurements in green, duplicate measurements not included)

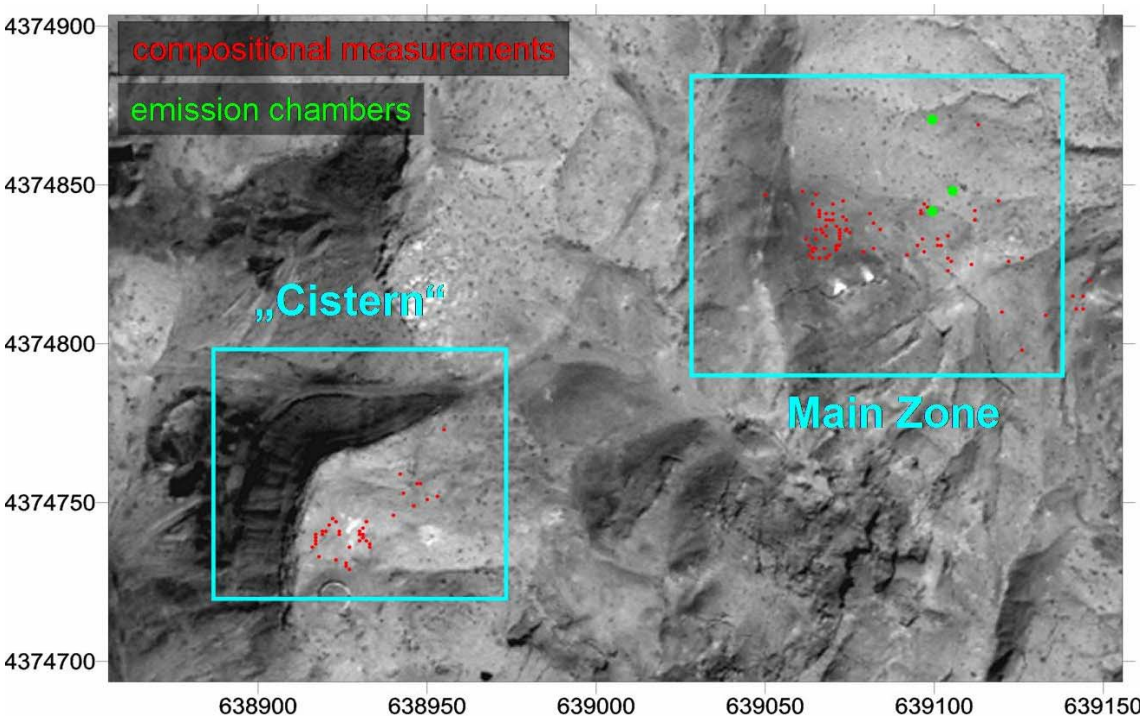

Figure 3: Sample locations at fire zone 8 with indication of the two different areas “cistern“ and “main zone“ (compositional measurements in red, emission chamber measurements in green, duplicate measurements not included)

On the northern part of fire 8 a large crack system exists, where 31 measurements were performed on July 1st, 2004. A day later, on July 2nd, completely different wind

conditions were observed, so that all measurements have been repeated on that day. On July 4th, very strong wind (average wind speed 8-10 m/s, gusts 12-15 m/s) occurred and it was impossible to get reliable samples from larger cracks and holes. At that day, the lateral wind speed in the cracks was measured in the 31 cracks measured the days before and additional 24 cracks.

4.2. Analytical Procedures

The application of a portable gas detection instrument (Draeger Multiwarn II) has proven to be a rapid and reliable method during the summer field campaign. This instrument was equipped with a CO_2 IR-sensor, a catalytical sensor (combustible gases) and chemical sensors for CO, H_2S and O_2.However particular attention must be paid to cross sensitivities and the environmental conditions (i. e. dust and ambient temperature). During the field work problems occurred with parts of the electronic equipment due to the high temperatures (e. g. failure of displays) but problems could be solved during the field campaign. Many of the compositional measurement had to be performed as a dilution of the vent gases (using air), ranging from app. 1:1 to 1:50 sample to air ratio. This was necessary for two reasons:

- to dilute the sample to concentration ranges where the chemical sensors for CO (max. concentration 500 ppm) and H_2S (upper limit 500 ppm) can work.
- Protect the sensors from capacity overload (H_2S, CO) and to avoid a corrosion of the CAT Ex sensor, which is highly sensitive to H_2S values in excess of 100 ppm.

However, after the first evaluation it became evident that the results of the O_2 sensor are not very feasible. The sensor has a sensitivity of 0.1% absolute. In many instances a dilution of approximately 25:1 (air: sample) had to be applied. A typical result would yield 0.41 % CO_2 and 20.6 % O_2. Table 1 shows the results of the calculation of this sample. The second row („potential deviation“) reports the calculated data assuming an error of the instrument at the last shown digit. It becomes very clear, that the CO_2 data (and the CAT Ex, CO, H_2S values) are reliable, whereas for oxygen a larger error has to be assumed.

Table 1: Calculation of true concentrations and related errors

	CO_2 response [%]	CO_2 calculated [%]	O_2 response [%]	O_2 calculated [%]
reported value	0.41	9.1	20.6	13.3
potential deviation	0.40	8.9	20.5	10.8
	0.42	9.4	20.7	15.8

The CAT Ex sensor for combustible gases sensor is highly sensitive to humidity, in particular if water can condensate on the sensor. Despite the fact that a water condensation flask was used, it cannot be completely ruled out that water might have condensated on the catalytic surface of the sensor resulting in an erroneous indication of combustible components in the vent gases.

4.3. Emission measurements

In principle, compositional gas measuring techniques fall in two main categories: soil gas and fracture measuring. Soil gas measuring yields the concentration of gases in the vapor space of soils, fracture measurement determines the gases which are released from a particular source, such as surfaces or cracks. Soil gas measurements are typically applied to outline focal points of emissions (e.g. detection of large fault zones by means of He anomalies) and are performed one- (transect) or two-dimensional. As well the emission through the soil (by means of emission chambers) as the flux rates in fractures or cracks (e.g. heat or vane anemometers) can be determined.

Soil gas flux measurements are used since several decades. They have been applied within the framework of Greenhouse gas emissions and soil dynamics as well as in volcanic fields and other geothermal areas (e.g. Cardellini et al. 2003; Bergfeld et al. 2001). A number of different techniques can be employed for gas flow measurements. These include micrometeorological methods, open or flow-through and closed chamber methods, which can be further divided into active or passive sampling methods (see Welles et al. 2001 for a brief review).

Classical collection of soil gas probes by means of steel pipes was not possible in the Wuda area (no or sparse soil/sand cover), therefore classical emission chambers were used which allow for compositional and flux measurements. All emission measurements were done using closed chamber (a passive method). The principle of the measurement using a closed “flux chamber” is relatively simple. A circular chamber (cylinder), made of steel or temperature resistant Plexiglas (Figure 4), with in- and outlet connectors is placed leak-tight on the soil and the concentration increase (or decrease in case of a gas sink) is measured as a function of time (Figure 5).

To ensure a constant homogenization of the gas in the flux chamber a small vane is placed in the chamber or the gas is circulated through the chamber and the measurement device by an internal pump. The frequency of data acquisition is depending on gas flow from below, ranging between 1sec intervals (for very high gas flow rates) and 15-30 minutes intervals (measurements of undisturbed soil). The concentration of the gas in the chamber is increasing in two phases. During the first phase the increase is linear with time and during the second phase asymptotically approaches a maximum value (saturation of the chamber). The gas flow from the soil or vent is determined from the linear increasing concentration by the following relationship:

$$Q = \frac{dc}{dt} \cdot \frac{V_C}{A_C} = \frac{dc}{dt} \cdot h_C$$

with dc/dt concentration increase over time, h_C height of the chamber and V_C, A_C volume and base area of the chamber respectively. The unit of the gas flow Q is $[Mass][Area]^{-2}[Time]^{-1}$. The gas concentration was determined with the portable multi-gas instrument Draeger Multiwarn II. High emission rates require high sampling frequency when using flux chambers (to record the phase of linear concentration increase). This limits the maximum flow rate which can be determined by this method. Highest sampling frequency with the detector is $1s^{-1}$. This results in a maximum determinable flow rate of approximately $1m^3/s/m^2$.

Figure 4: Plexiglas emission chamber with multi-gas instrument Multiwarn II (internal pump circulating the gas) and temperature measurement at fire zone 3_2

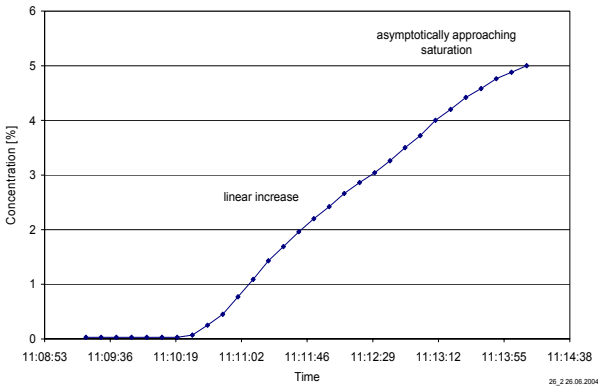

Figure 5: Concentration increase in a flow chamber as a function of time

Heat wire anemometers (usable up to a temperature of 80°C) and vane anemometers are only from very limited use. The small vents or fractures do not allow exact vertical alignment of the instrument relative to the gas flow direction. Therefore reliable and reproducible measurements are hardly possible. Differential pressure measurements using a Pitot-static tube as used by DMT/Uni Würzburg have proven to be the best method of choice in high temperature / high velocity environments.

The emission chamber has been used on small, well defined gas emitting fractures and holes as well as on sites with no visible emission structures (hereafter simply described as “soil measurements”, Figure 6). The total absolute emissions of gas from the small fractures and holes at fire zone 3.2 range between 0.01 and 6.2 m³/day. A hole with a diameter of 0.5 cm has an area of 0.0000196 m², the largest measured cracks had a dimension of 5cm * 20cm equal to an area of 0.01 m². When the gas flow are normalized to a gas emission rate per m² these values increase by several orders of magnitude (4 – 114000 m³/day/m², average is about 10000m³/day/m², Figure 7). Compared to this, the emission rates of areas with a sand cover range between 0.006 and 12 m³/day/m² (average 2.2 m³/day/m²). It is important to note, that these areas in fire zone 3.2 represent an artificial coverage of larger fractures and other exhaustion areas. The flow rates might not be typical for gas emissions through an undisturbed matrix of the overlying rocks. Litschke et al. (submitted) presented a rough estimation of gas emissions at FZ 3.2 using all available data for this site. The estimate a CO_2 emission between 729 and 953 kg/h.

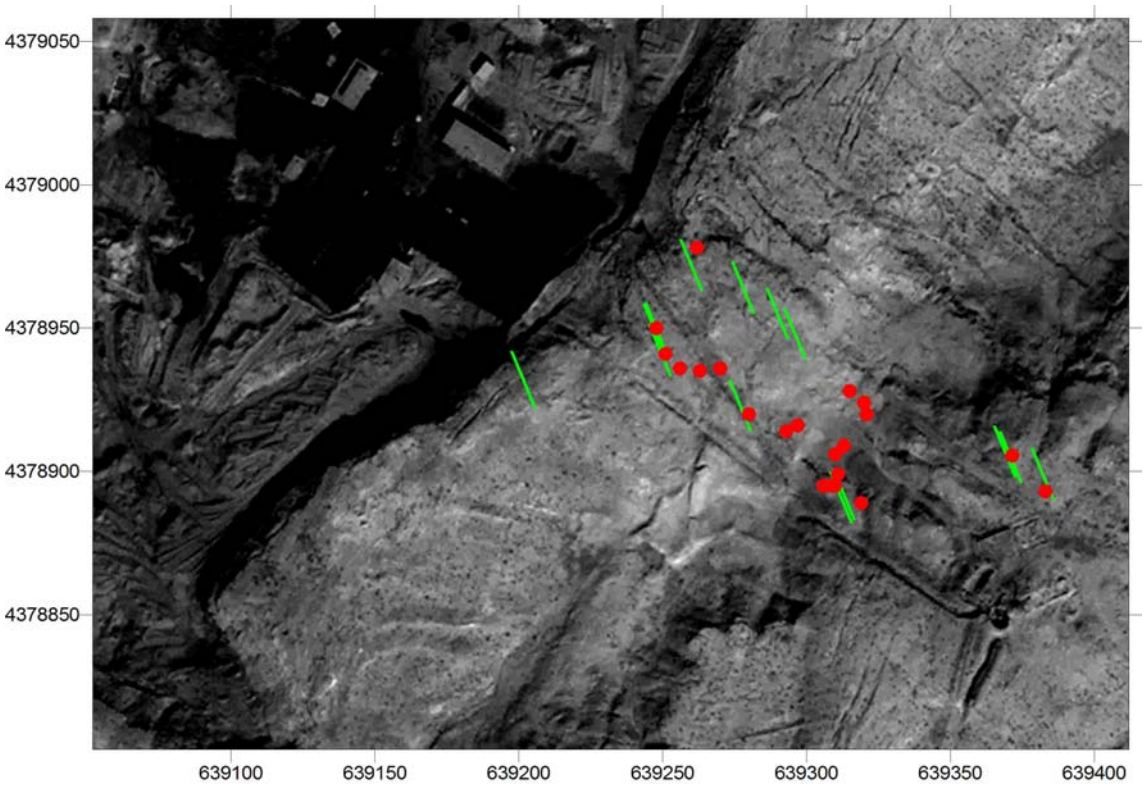

Figure 6: Locations of soil (red dots) and fracture/hole flow measurements (green lines) at fire zone 3.2

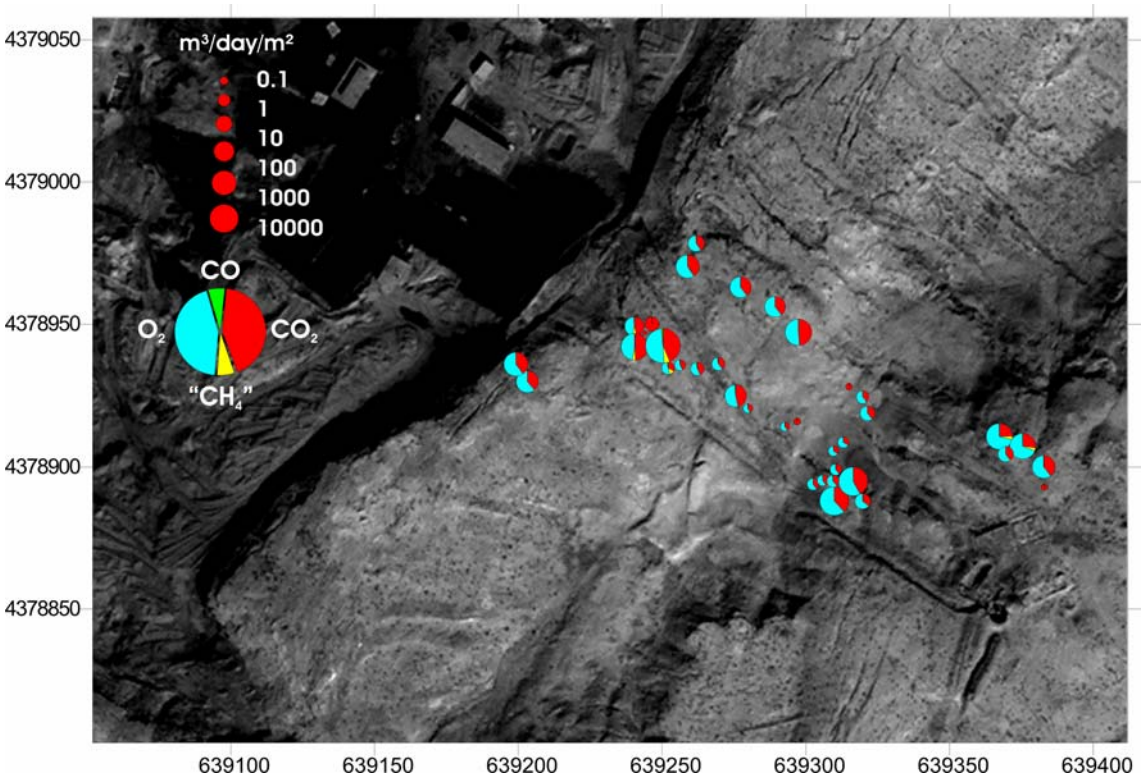

Figure 7: Total gas emissions of fractures/holes and through the sand cover. Note, that data are normalized per square meter and the scale is logarithmic

A 1-dimensional transect was measured at one location (fire zone 3.2, between the main vent zones) where the fire is artificially covered by a sand/soil mixture. Between two main ventilation zones (large cracks) the gas emissions through the sand cover were measured (Figure 8). Despite the coverage with relatively fine grained sediments

(pers. comm. Fire Fighting Department in Wuda) substantial emission rates up to 1m³/m²/day could be recorded. This value is up to three orders of magnitude higher than typical CO_2 desert soil gas emissions (~4 gCO_2/m^2/day, Parker et al. 1983).

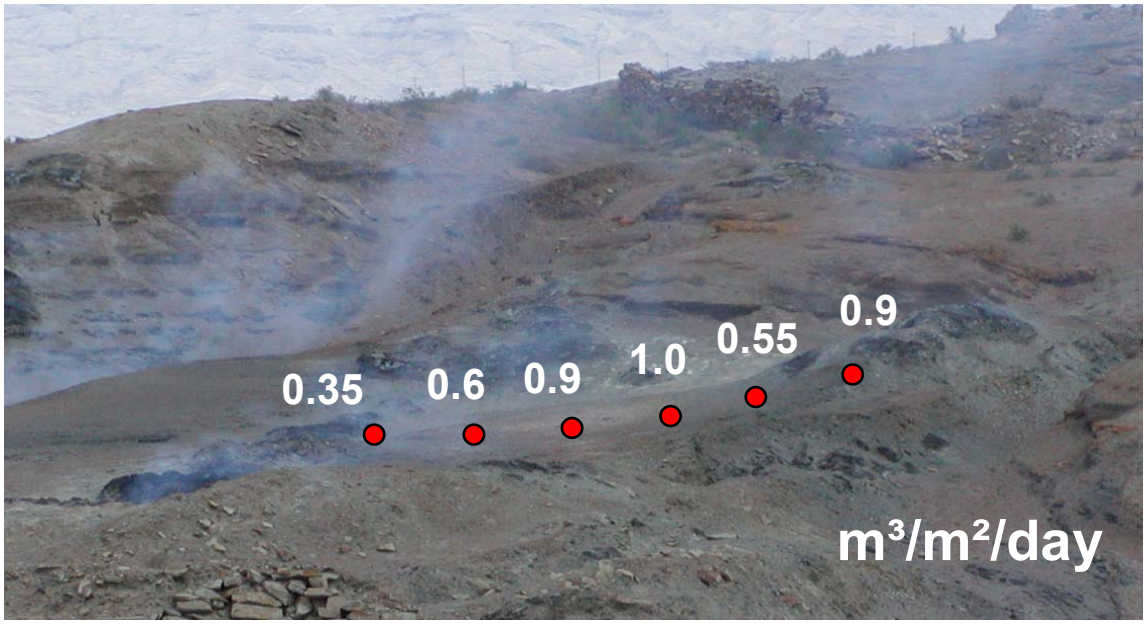

Figure 8: Gas emissions through the artificial coverage at fire zone 3.2 (Background Image courtesy GGA)

4.4. Compositional Measurements

4.4.1. Fire 3.2

CO_2 ranges from 0 to 16.3%, "CH_4" (CAT Ex Sensor) from 0 to 0.5%, O_2 from 0.6 to 20.9%, CO from 0 to 9462 ppm and H_2S from 0 to 684 ppm (Figure 9). The sum of O_2 and CO_2 does not always account for the theoretical value of 20.9%. The value varies between 11% and 23.7% (average 19.2%). This is partly due to the error introduced with the dilution of the sample (see above, chapter 4.2) but also reflects the high water vapor content of the combustion gases. At 85°C a gas saturated with water vapor contents about 350 g/m³ (which is approximately 65% of the overall exhausting gas).

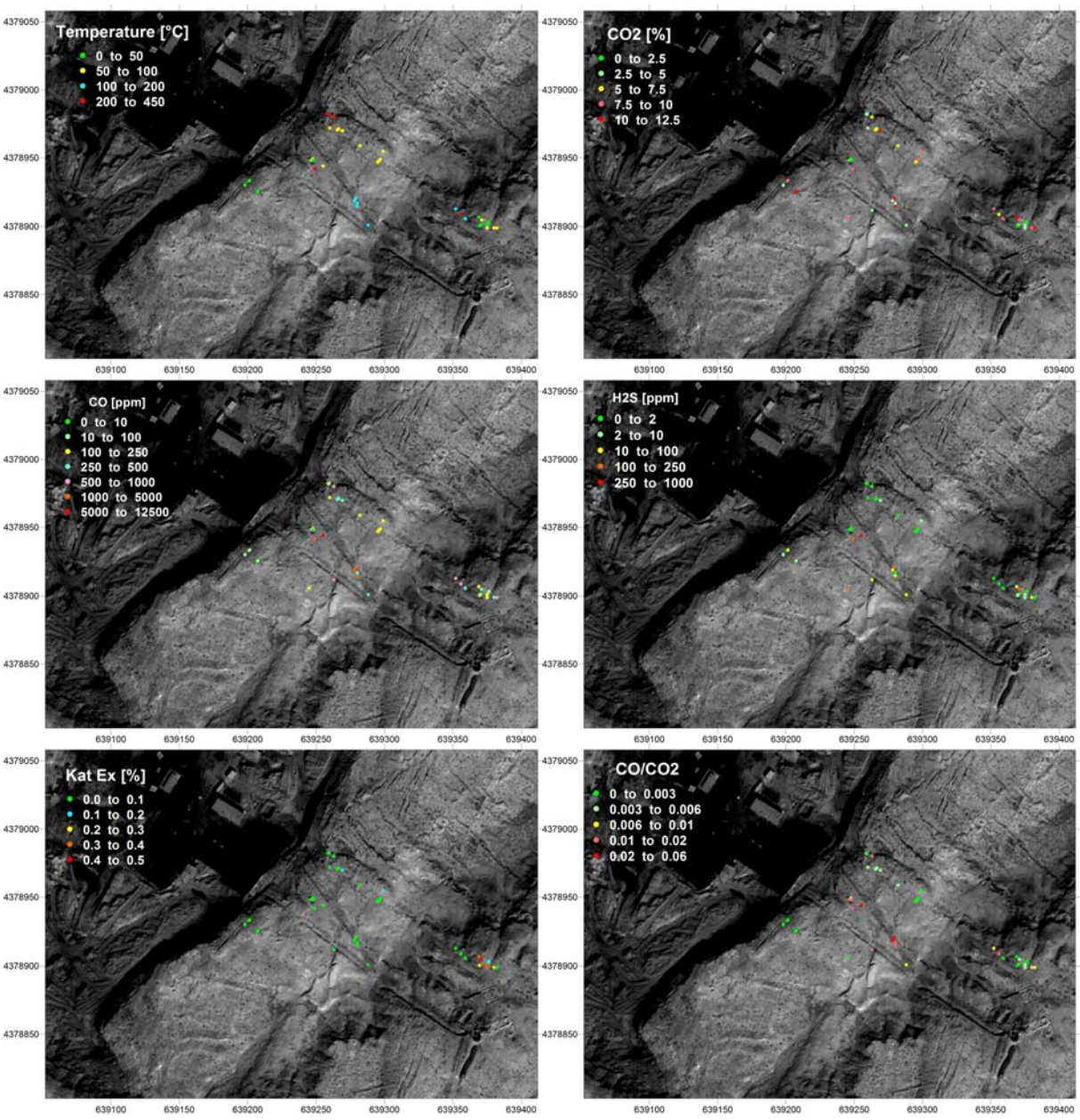

Figure 9: Composition of gas emissions and corresponding CO/CO_2 ratio at fire zone 3.2

4.4.2. Fire 8

Fire 8 has been divided into two different zones, the main zone and the area around an old water cistern approximately 200m to the SE from the main zone. The latter zone exhibits only smaller cracks with relatively low temperatures. CO_2 ranges from 0.03 to 1.4%, CO from 0 to 307 ppm and H_2S from 0 to 9 ppm (Figure 10). Methane, i.e. CAT Ex Sensor, was not detectable in this zone.

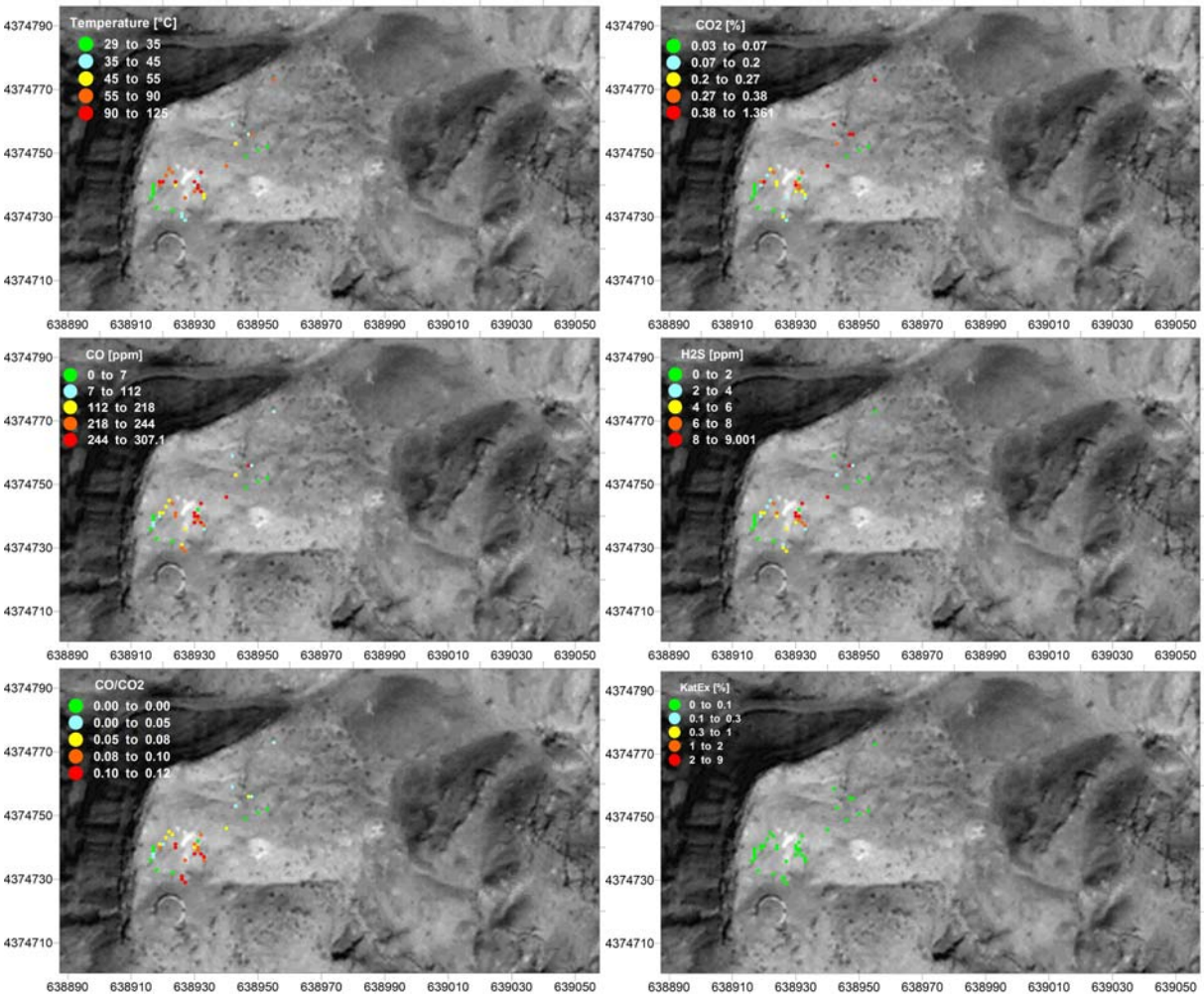

Figure 10: Composition of gas emissions and corresponding CO/CO_2 ratio at fire zone 8, "cistern". Note that no methane/flammable gases have been detected.

4.4.3. Discussion and Interpretation

The main zone is characterized by higher temperatures of the ventilation zones. CO_2 ranges from 0.03 to 7.8%, CO from 0 to 17500 ppm and H_2S from 0 to 900 ppm and methane up to 9% (Figure 11). Data suggest that there is a small area close to the main ventilation zone where higher CO and CH_4 contents have been measured. This "halo" is possibly related to the advancing front end of the fire zone where the aforementioned process of pyrolysis in a low temperature regime occurs. This zone is very small and extends only for several meters, but that corresponds to the normal and typical extension of elevated temperatures. Huang et al. (2001), Yang (2004) and Klika et al. (2004) have shown, that the extension of higher temperatures close to the fire area is very limited (maximum some tenths of meters).

It becomes evident, that the fire zones among themselves are very inhomogeneous in terms of temperature and gas composition (Figure 9, Figure 10, Figure 11). Also fire zone 3.2 compared to fire 8 is clearly different. Methane contents are generally lower in fire zone 3.2 (Figure 12) and the CO/CO_2 ratio are different as well (Figure 13). The difference between the two studied fire zones (and the defined "subzones") becomes furthermore evident after a statistical evaluation of the data (cluster analysis, Figure 14). Compositional data show distinct clustering with the exception of the gases originating from the burning seam 9 at fire zone 3.2.

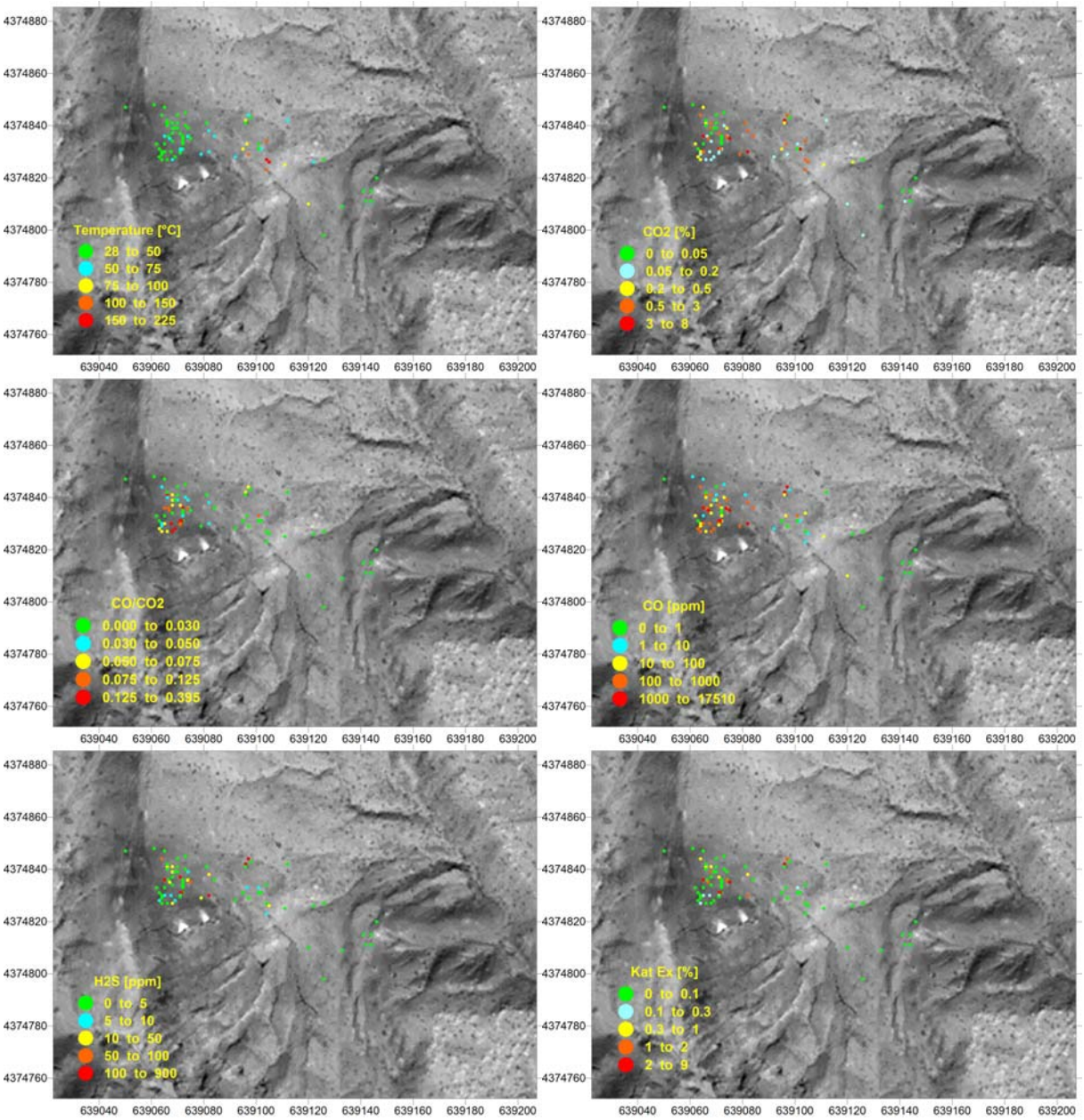

Figure 11: Composition of gas emissions and corresponding CO/CO_2 ratio at fire zone 8, main zone

Gas composition as a combustion indicator has been used to monitor abandoned coal mines (Kim & Chaiken, 1993). However, the composition of the gases at the surface depends on many different factors: combustion process, migration, differential pressure, temperature (gradients) and dilution of the gases. Therefore it is not surprising that no clear relationship between temperature of the gases and the respective chemical composition could be established. CO, H_2S and CO_2 do not vary systematically with temperature (not shown). Methane seems to be restricted to low temperature ventilation zones. The oxygen content is inversely proportional to the CO_2 content, but independent of the temperature. Combustion products of underground fires have often yielded ambiguous results (Kim & Chaiken, 1993). Due to limited compositional data (N_2 not determined, O_2 data partly inaccurate) only the CO/CO_2 and O_2/CO_2 ratio as a function of temperature could be evaluated for the areas under investigation. None of these ratios depends on the temperature of the gases (Figure

15, Figure 16), indicating that the gases emanating at the surface are at least partly diluted by fresh air.

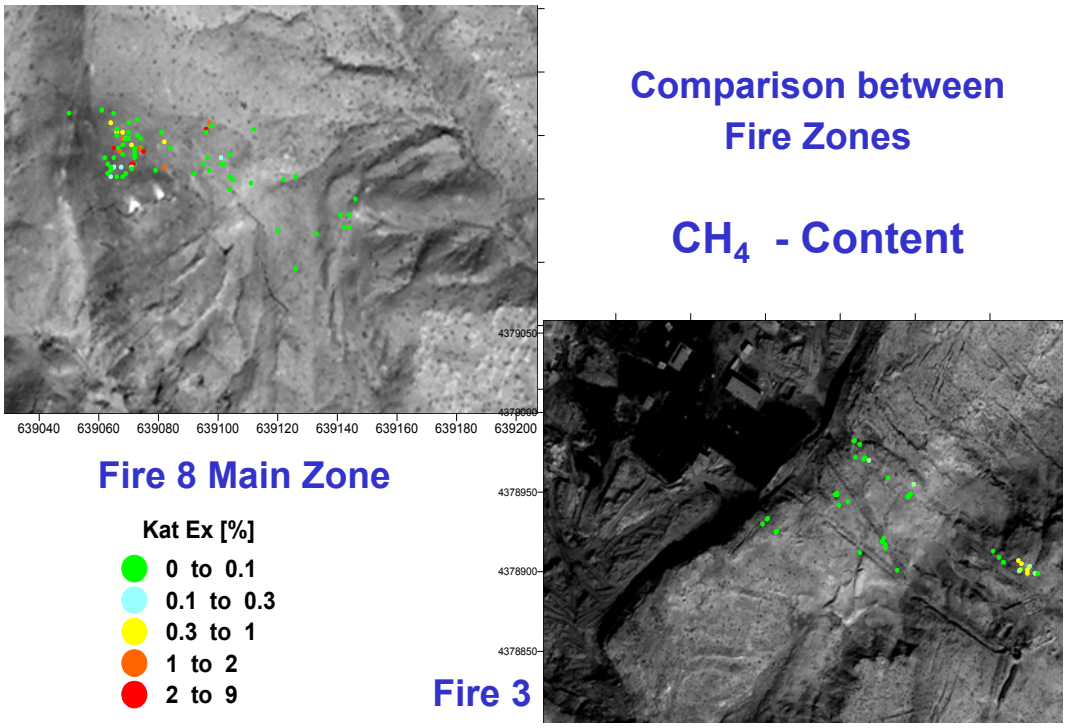

Figure 12: Comparison of methane in gas emissions of fire zone 8 (main zone) and fire 3.2. No methane was detected at fire 8 „cistern“

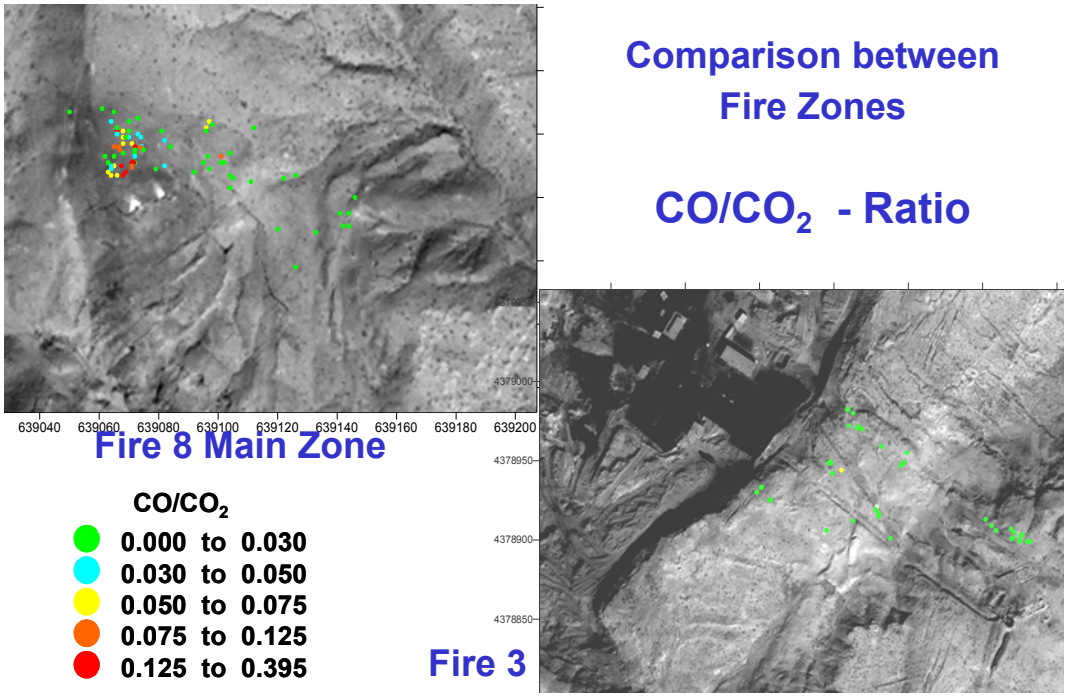

Figure 13: Comparison of the CO/CO2 ratio in gas emissions of fire zone 8 (main zone) and fire 3.2.

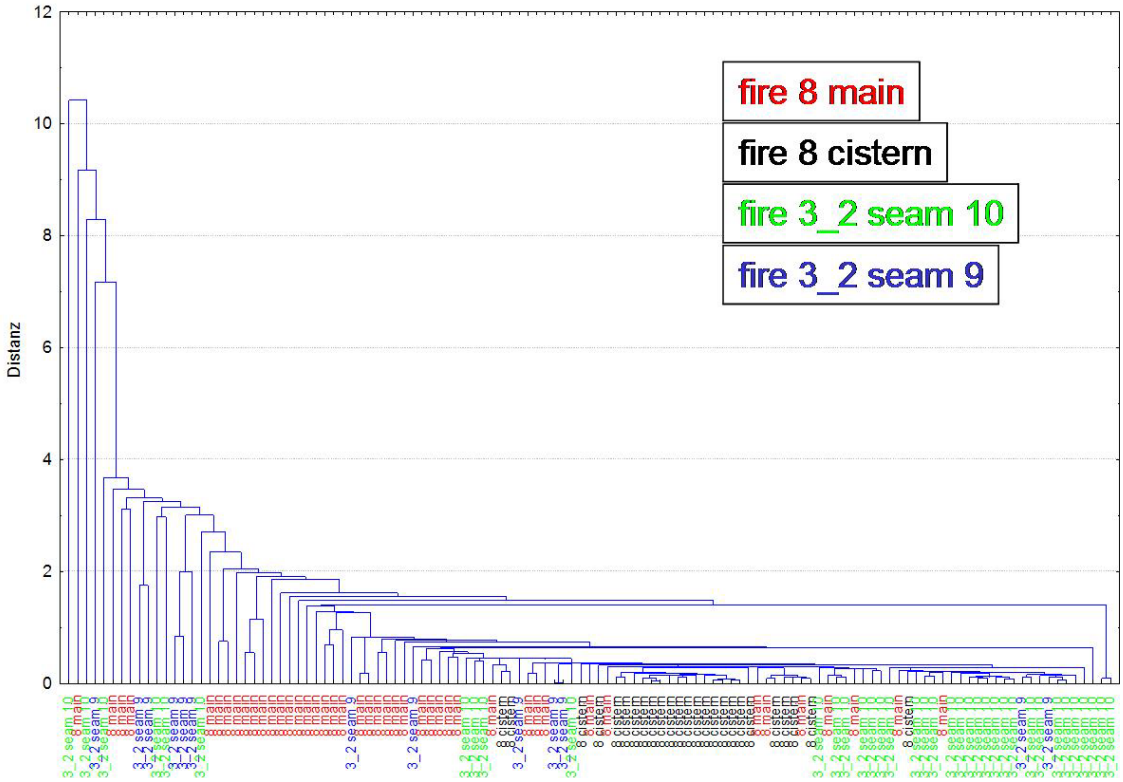

Figure 14: Cluster analysis of compositional data

The Bureau of Mines (US Department of the Interior) has developed a diagnostic hydrocarbon index, to detect hot and cold subsurface zones by means of inter-borehole communication test (Dalverny & Chaiken, 1991; Kim, 1986, 1991). The index, basically the molar fraction of higher hydrocarbons, is based on the fact, that with increasing temperature more heavier hydrocarbons are released from the coal (desorption process). However, the absolute value of the index does not depend on the temperature but on type and rank of the coal (see above).

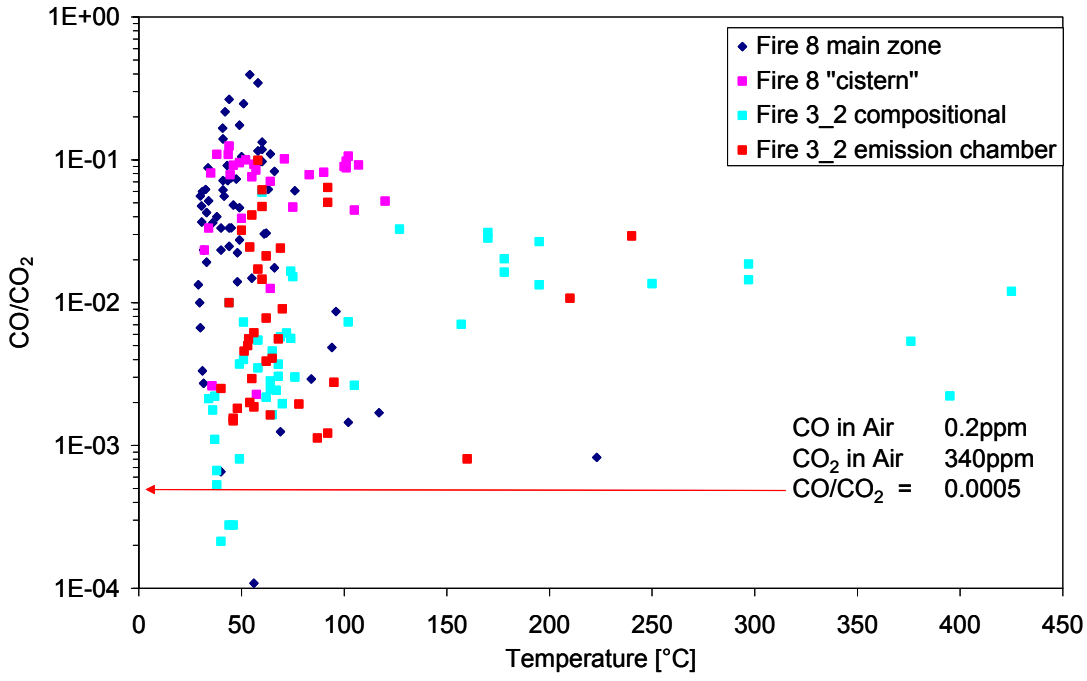

Figure 15: CO/CO_2 ratio versus Temperature

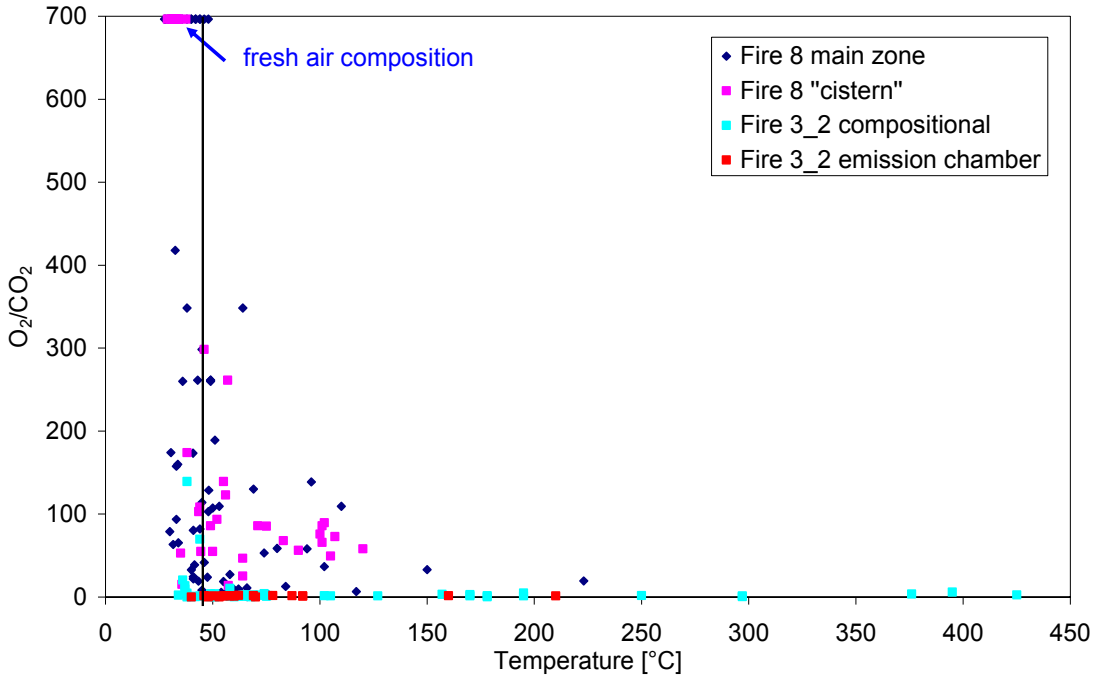

Figure 16: O_2/CO_2 ratio versus Temperature

A couple of samples have been analyzed in the BGR laboratory to provide evidence that in fact methane was detected by the catalytical sensor. The samples were taken a couple of days after the field measurements, so that total composition is not directly comparable. However, the GC analysis yielded CH_4 contents up to 1.5% and traces of higher hydrocarbons (up to 0.16%, Table 2).

In addition the occurrence of molecular hydrogen (H_2) in significant amounts was detected (up to 3.2%, Table 2). This indicates that the aforementioned reaction pathways similar to carbonization/gasification processes de facto occur. Hydrogen generation due hydrogen corrosion (reactions between acids and base metals) is a potential mechanism but it is unlikely to be the cause of H_2 occurrence since the gases have been only for a short time in contact with steel conduits during sampling.

Table 2: Results of GC measurements, concentratrions normalized to 100%

	N_2	O_2	CO_2	CO	H_2	CH_4	C2+
	[%]	[%]	[%]	[ppm]	[ppm]	[ppm]	[ppm]
Wuda 2	74.72	12.81	11.58	1185	5197	2403	96
Wuda 3	77.43	11.68	10.54	0	0	2946	510
Wuda 4	77.39	6.78	15.02	0	3152	4160	860
Wuda 5	69.95	11.3	13.68	1293	32136	15535	1679
Wuda 6	73.53	14.58	8.83	879	19838	8972	882
Wuda 7	75.89	18.76	2.81	2641	16677	5845	282

4.5. Influence of Wind on Measured Gas Concentrations

As mentioned earlier, 31 samples have been re-measured under different wind conditions at fire 8. It can be clearly said, that the wind direction and wind speed have a very strong influence in large cracks. With the strong wind (average 6-8m/s, gusts up to 12 m/s) from NW direction most of the CO_2 values are close or identical to air concentration (0.03%). Under different conditions (wind from SE direction, average 2-4 m/s with gusts up to 6 m/s) CO_2 and CO concentrations are usually much higher (Figure 18). Examination of the CO_2/CO ratio didn´t result in a more reliable interpretation (Figure 19).

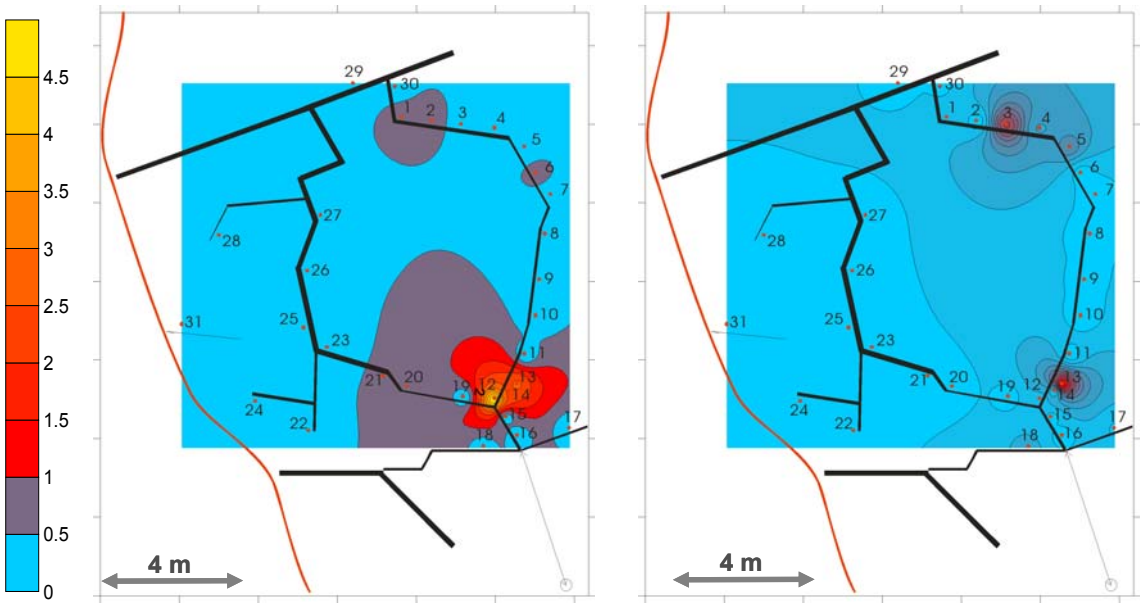

Figure 17: CO_2 (%) concentration depending on wind conditions (left: moderate wind from SE, right: strong wind),

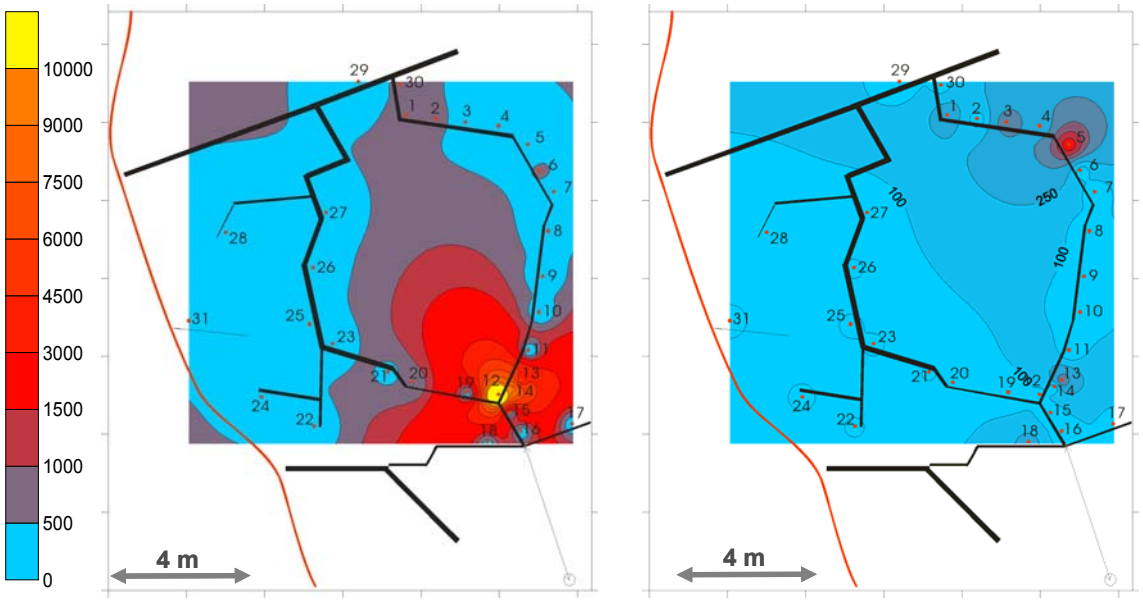

Figure 18: CO (ppm) concentration depending on wind conditions (left: moderate wind from SE, right: strong wind)

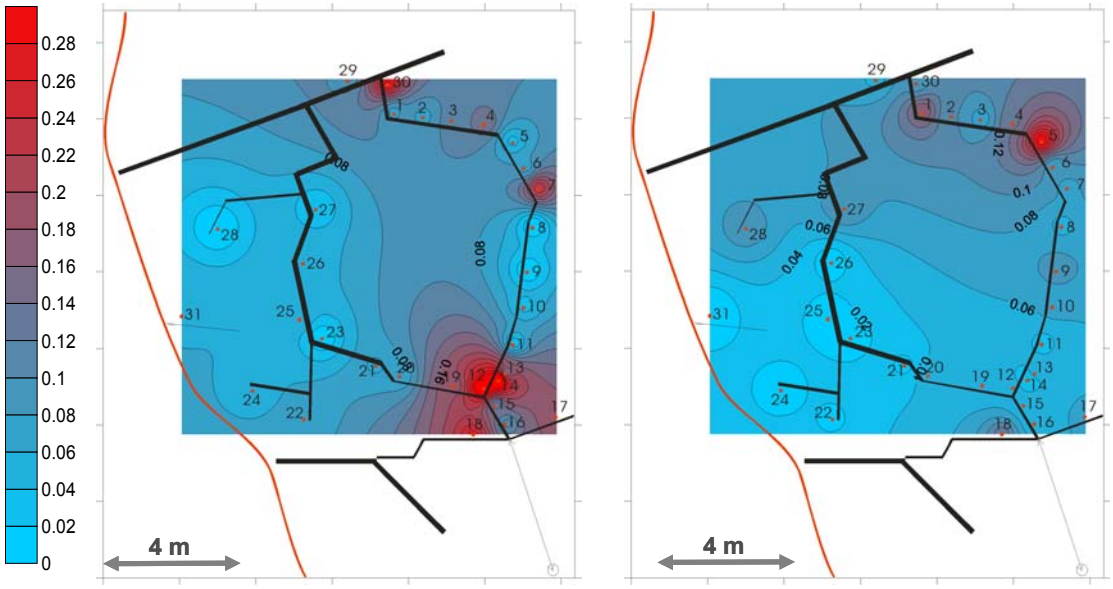

Figure 19: CO_2/CO ratio depending on wind conditions(left: moderate wind from SE, right: strong wind), black lines indicate the fracture system, numbers/red dots sample locations

On July 4th wind was coming again from NW with wind speeds ranging from 9-11m/s and gusts up to 16m/s. Under these conditions it was impossible to measure chemical composition of exhaustion gases. Therefore, the wind speed in the larger cracks has been determined. The heat wire anemometer was placed perpendicular to the axis of the crack in a depth of 30 cm (with a few exceptions). The strong wind caused strong air currents in the cracks. Three minute average values go up to 2.6m/s with maximum values going up to nearly 6m/s (Figure 20).

This technical expertise's strongly influenced the selection of the site for the continuous monitoring carried out during 2005 (see chapter 5).

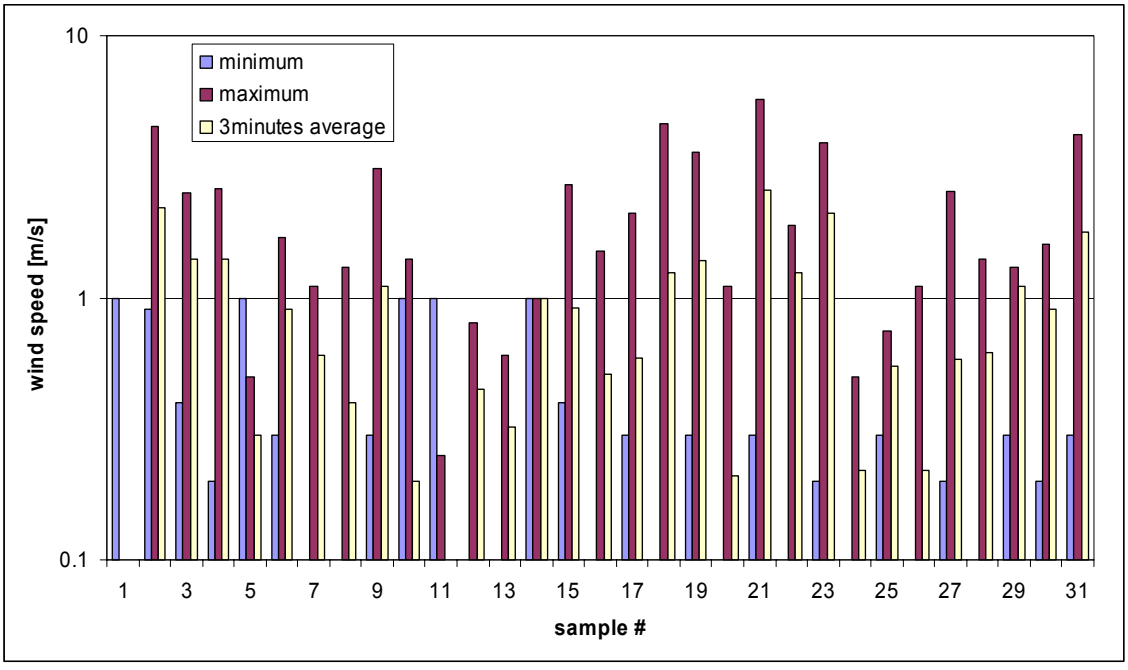

Figure 20: Lateral wind speeds in large fractures (dimension between 1 and 22cm) during a stormy day

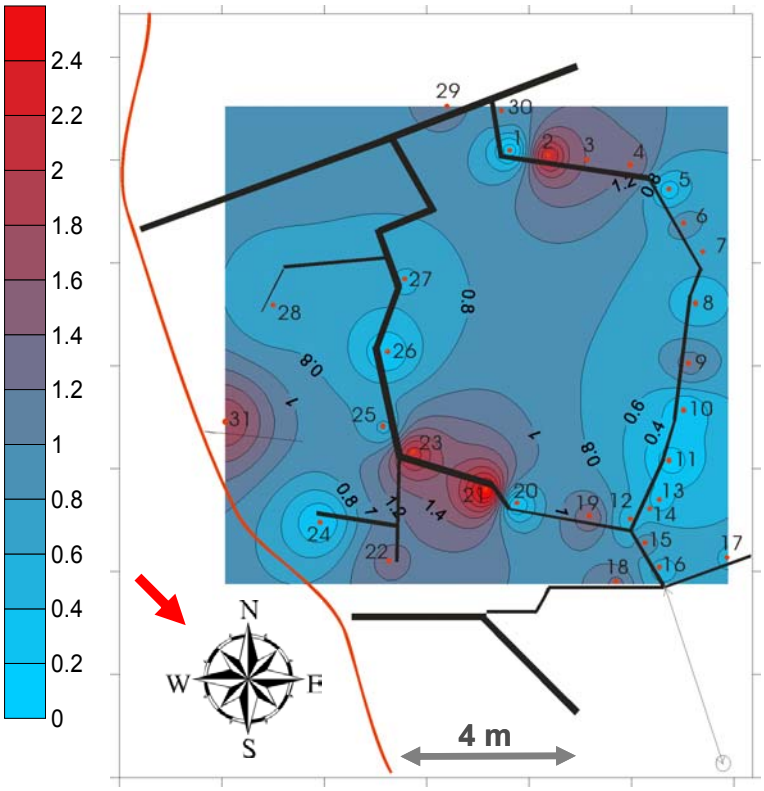

Figure 21: Lateral average wind speeds (m/s) in large fractures at fire zone 8. Red arrow indicates main wind direction

4.6. Summary Combustion Gas Analysis

In conclusion, the results from the combustion gas analysis can be summarized as follows:

- The fire zones among themselves are very inhomogeneous in terms of temperature and gas composition
- The fire zones compared to others are different
- No clear relationship between gas composition and temperature could be established
- Non-combustion products like hydrocarbons & hydrogen are detectable in significant amounts
- More than a simple combustion process is involved in natural coal fires (pyrolysis / carbonization, coal gasification), but the contribution of each process is unclear
- Besides the emissions from large fractures significant amounts of combustion gases reach the surface by migration through the matrix of the overlying rocks and/or a artificial covering
- Sites for gas and temperature measurements (either discontinuous or permanent) must be carefully chosen

5. Permanent Monitoring Station (WP 3430)

– Location, Initial Conditions and Technical design –

Fire zone 8 (FZ) was chosen jointly by DMT and BGR as the key measurement site because it offered the most suitable conditions compared to the other fire zones 3.2 and 11 selected for in-depth investigations. At FZ 8 no active fire fighting with water/mud injections and/or artificial covering took place, the geology and the geometry of the subsurface coal fire is fairly simple, many geological information were available by mapping and drilling, and extensive temperature and chemical measurements had been carried out in the earlier phases of the project. The long-term gas and temperature monitoring was installed during May/June 2005 and scheduled to be operated until October 2005. Parallel to this installation DMT operated a permanent micro-acoustic survey nearby with two seismometers in boreholes (20 and 10m depth) and two more at the surface (Figure 22). End of October, after the DMT flooding experiments had been supplemented with concomitant gas and temperature measurements of our group, the monitoring unit was de-installed due to customary regulations.

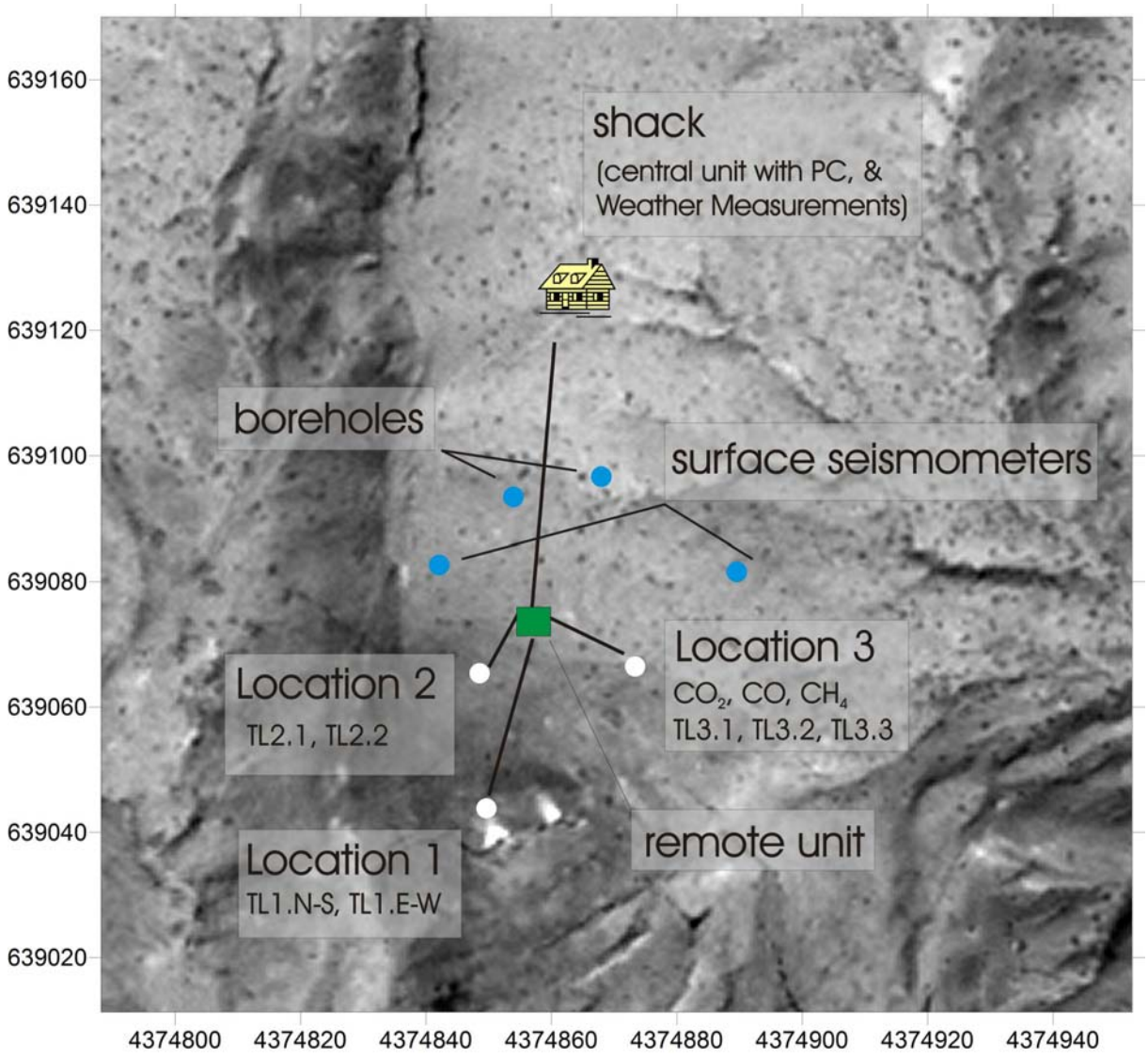

Figure 22: Location of the central unit in the shack, the remote unit and the three different measurements sites at FZ 8 (projection UTM 48 S (WGS84))

The system applied for this project was a modification of the BGR gas monitoring system, which has been continuously improved over the last years. Special emphasis has been placed on the design and development of an adapter for reproducibly sampling hot gases (T ≤ 110°C) having a high content of humidity and containing corrosive sulfur species. The system has been operated for extended periods of time (i.e. months, years), e.g. at Galeras volcano (Colombia) and at Nisyros hydrothermal vents (Greece), similar systems are further in use for monitoring earthquake precursors. Software has been developed for instrument control, data acquisition with cycle times of seconds, data storage and on-line telemetry if necessary.

The Wuda Coal Fire permanent multi-parameter station consisted of two units. The central processing and data acquisition unit which was based in a newly built shack and the remote (outdoor installation) unit which was located close to the main fire zone (app. 15m).

The central unit consisted of the main power supply, the controlling computer (PC/104), one data logger and the installations for the meteorological measurements. Power supply at remote location is usually provided by solar panels in remote locations, but at the chosen location at FZ 8 electricity power supply was made available by the Wuda Coal Mine. However, the system, operated at 24V, was backed up by two 12V looped-in and constantly charged batteries allowing for a maximum downtime of 10 hours of the main of 220V power supply.

The data logger was a Gantner Instruments ISM 111 (4 analog inputs 16 bit ADC and 4 digital in/outputs) used for A/D conversion of the signals from the wind vane, wind anemometer, ambient temperature, barometric pressure and battery voltage. The accuracy of the wind anemometer is ±0.5% (min. 0.6m/s) and for the wind direction sensor 7° at 0.6m/s. Barometric pressure was measured with a Cerabar T PMC 131 pressure sensor (long-term stability ±0.15%/year, accuracy ± 0.5%). The controlling computer was equipped with a GSM modem for daily data transmission to Germany (offering a *real time monitoring*) and software to control all components from remote places. All data from the ISM 111 logger were stored on the computer hard disk.

The distance of the remote unit from the shack was about 70 m. The communication lines running from and to the remote station (Teflon® tubing for the gas and control lines) were placed in plastic tubes (5cm Ø) for protection against external damage. The remote unit consisted of two 2 Gantner IDL100 data loggers (8 analog inputs 16 bit ADC, 6 digital in/outputs, 256 KB internal RAM and a 8 MB PCMCIA Flash memory card), mass flowmeters (TSI, accuracy ± 2%), miniature diaphragm air pumps (maximum flow rate 1.2 l/min), IR gas sensors and a thermocouple for temperature measurement in the equipment box. All loggers and flow rate regulators (2 channel D/A converter) were connected via a RS 485 fieldbus interface to the controlling computer in the central unit. All sensors, loggers, flow meters and pumps were assembled in water- and dust-protected cases (IP 67).

Three different fracture locations were monitored by the remote station (Figure 22).

5.1. Location 1

Location 1 is located close the main combustion zone 20m off the remote unit. The Type K thermocouples (50cm long, with ceramic protective tube) were placed in two 15cm wide cracks orientated almost vertically (consecutively termed *TL1.N-S* and *TL1.E-W*, Figure 23). White precipitations of calcite or gypsum/anhydrite were observed at these fractures, but no traces of elemental sulfur. The thermocouples were placed in a depth of app. 50cm, well-protected from direct wind influence and connected by a thermocouple compensating line to the data logger. In June 2005 the actual temperature of T1.N-S was 350°C and of T1.E-W it was 400°C (see below). In a distance of about 3 m to the South temperatures in excess of 750°C were measured and in another nearby large crack red-hot bedrock can be observed in a depth of a few meters. The glowing bedrock is clearly a result of the secondary combustion process, because the coal seam is much deeper at this specific location.

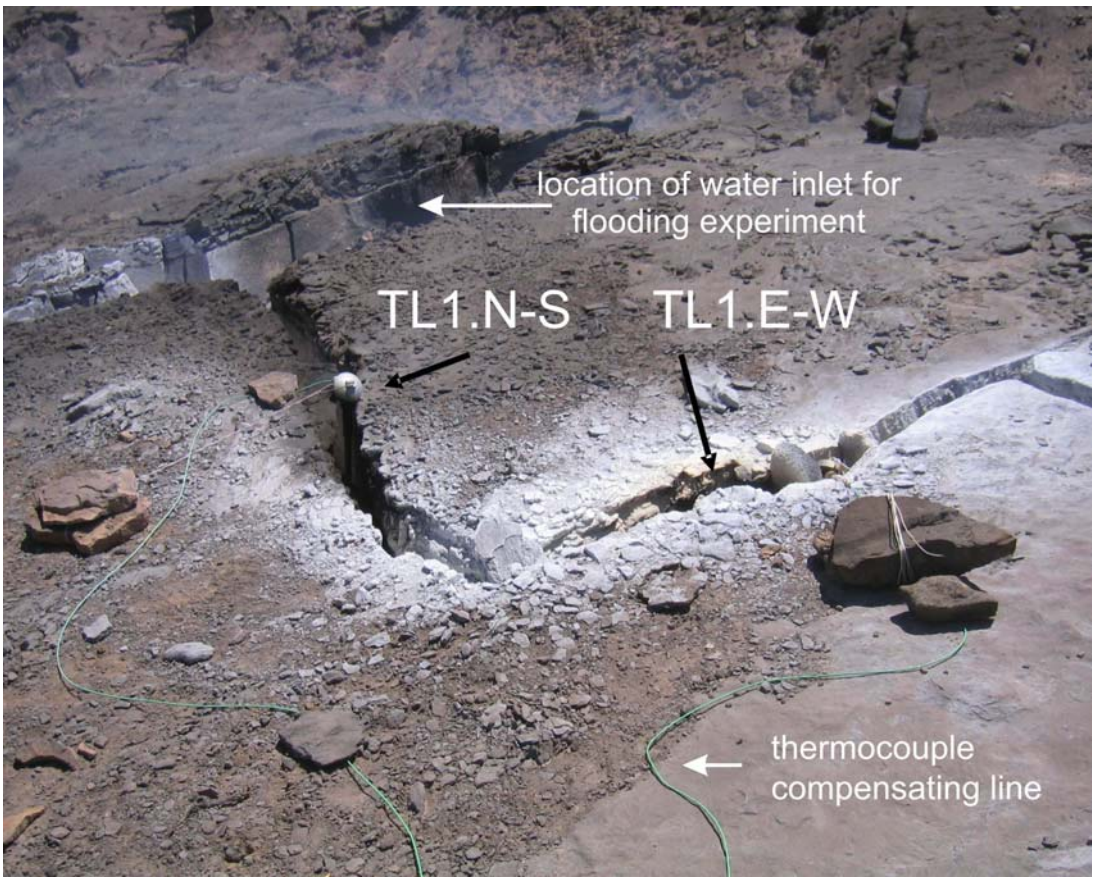

Figure 23: Two high temperature measurements were installed in a N-S and E-W trending fracture in very close vicinity to the main combustion zone

5.2. Location 2

Location 2 represents a low temperature (75°C, Figure 24) gas emanation equally distant from main combustion zone like location 3. One Teflon® insulated Pt-100 thermocouple was installed at the beginning of the monitoring period (June 2005) at site TL2.1, the second one October 18th, 2005 at site TL2.2. The thermocouples were inserted into the fractures to a depth of about 75cm. Location TL2.1 is a small vent (several cm in diameter) but seems to be part of a large discontinuous fracture. Around this vent the typical condensation products (i.e. tar and waxy hydrocarbons)

are staining the surface rocks. The vent gases at his site (measured in June 2005, standard laboratory conditions) comprised ~7.7% H_2, 61% N_2, 25.5% CO_2, 1% CO, 2% CH_4, 1000 ppm ethane and traces of higher hydrocarbons (saturated and unsaturated compounds). TL2.2 is part of a larger and deeper fracture, which can continuously be traced to the main combustion zone. No gas composition was determined at this site. Although the thermocouple was placed in a depth of app. 75 cm the temperature profile measured from October 19th – October 26th showed a clear dependence of wind direction (Figure 25). This variation has to be considered as an effect result of lateral influx of fresh air into the fracture and is not on indication of changing combustion efficiency.

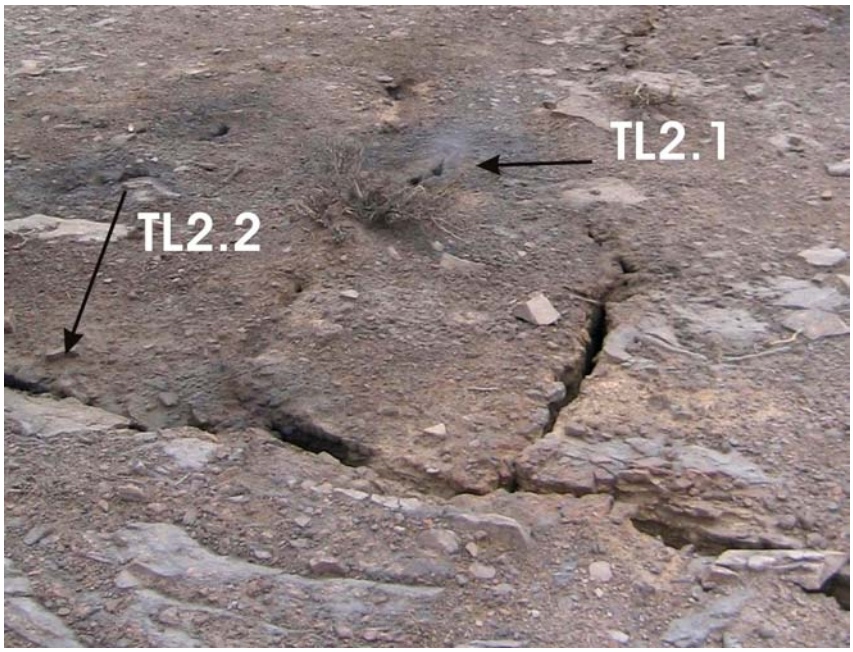

Figure 24: Location of low temperature measurements (TL2.1 June-October 2005, TL2.2 October 2005)

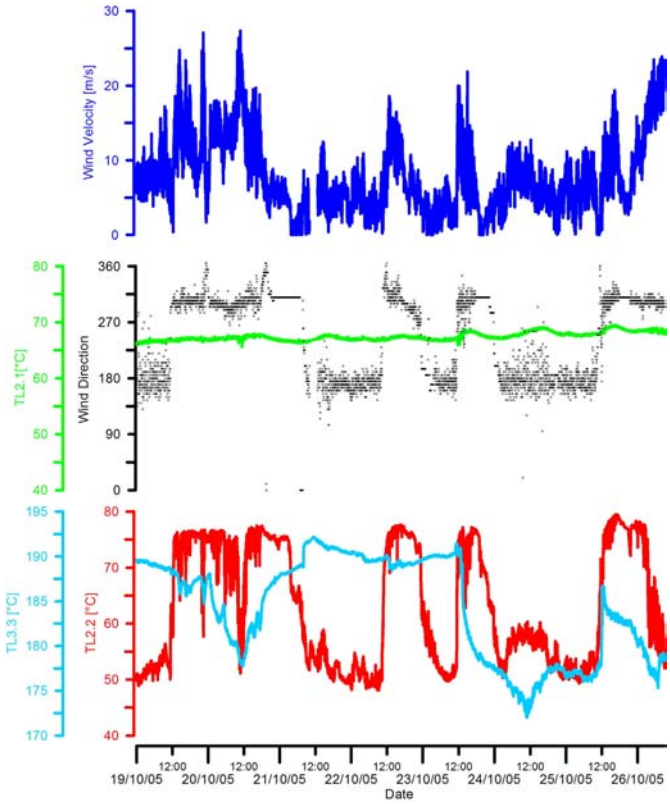

Figure 25: Temperature profile of TL2.1, TL2.2 and TL3.3 from October 19th - 26th, showing a well-defined correlation between wind direction and temperature for TL2.2 (red), TL2.1 (green) and TL3.3 (light blue) are not influenced

5.3. Location 3

At **location 3** (Figure 26) both gas composition (CO_2, CO, CH_4) and temperatures were measured. The emanating gas was diluted by a two-step system, consisting of a primary membrane in the vent and a secondary exchanger/diluter, a modification of patented system according to Poggenburg & Faber 2004. The combustion gases are pumped to the secondary exchanger, Figure 26). After the dilution step the gas moves to the IR-sensors. In this stage, the steam content of the combustion gases is for the most part removed due to condensation and the gas concentration is well within the measuring range of sensors. The dilution factor was determined during installation and has a value of about five. All results shown later are uncorrected measured values and not yet compensated for the dilution. The exact calibration is part of the ongoing work.

For the gas measurements IR sensors were used (Pewatron Carbondio and Gas Module). The measuring range for the CO_2 and CH_4 sensor was 0-10%, for the CO sensor 0-30000 ppm (accuracy ± 2% for all sensors). Intentionally it was planned to measure also molecular H_2 with a semiconductor sensor. However, after the dilution of the measuring gas the sensor signal was still higher or close to the maximum range (10000 ppm H_2) and therefore the H_2 detector was removed. The semiconductor sensor used showed some cross-sensitivity for other combustible gases (e.g. CH_4, C_2H_6). The high value was clearly a result of the elevated hydrogen concentrations and the cross-sensitivity of the sensor to these components. The flow rates were controlled by two miniature diaphragm gas pumps and constantly verified by mass flowmeters.

The sampling location is part of a long extending E-W directing fracture, which is close to the main combustion zone (approximately 15m apart). Temperatures vary strongly in this fracture. At measuring site TL3.1, where also the gases were extracted, the initial temperature in June 2005 was 78°C. The gas composition (measured at standard P-T laboratory conditions) at this time was ~10%H_2, 59%N_2, 22% CO_2, 3.8% CO, 3.2% CH_4, 1400 ppm ethane and traces of higher hydrocarbons (saturated and unsaturated compounds).

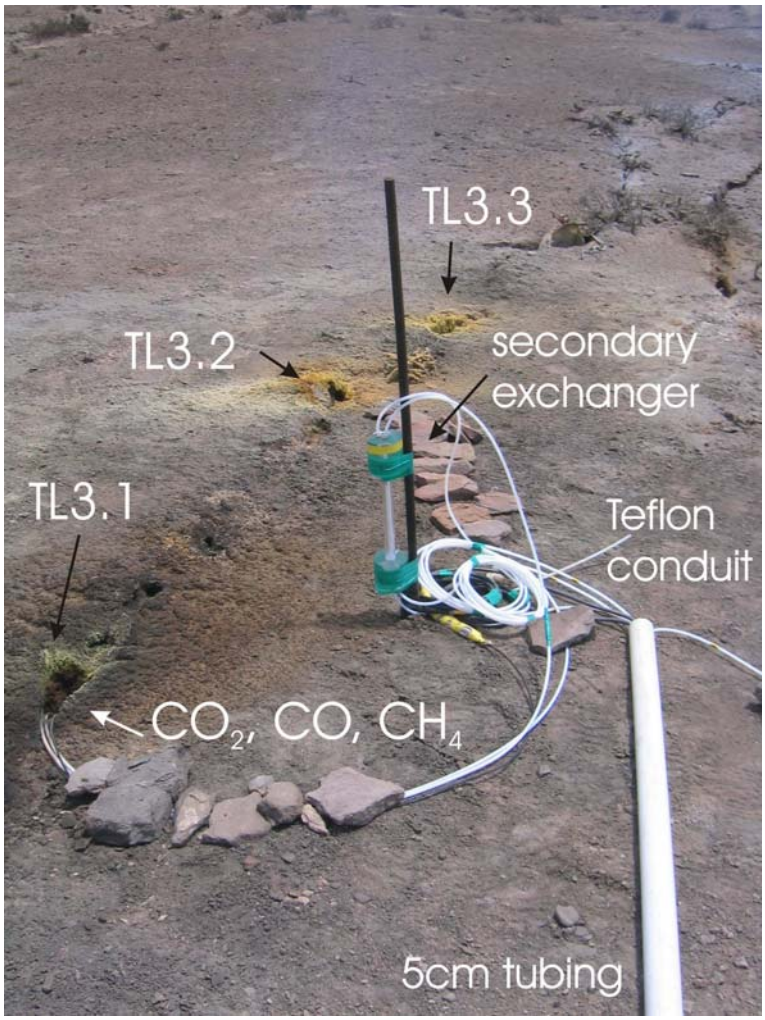

Figure 26: Overview of location 3 with temperature measurements (TL3.1 & TL3.2 June – October 2005, TL3.3 October 2005), tubing and secondary exchanger

At the site TL3.2 the initial temperature was much higher (150°C), although the site belongs to the same fracture and is very close to location TL3.1 (distance less than 1.5m). The different outlet temperatures were also reflected by the different precipitations around the vents. The lower temperature vent TL3.1 showed more dark colored organic condensation products with only minor amounts of sulfur, whereas TL3.2 as well as TL3.3 (temperature measurement only during the flooding experiments in October 2005) were clearly dominated by sulfur-rich depositions (Figure 26).

In total 15 different parameters have been recorded with a time resolution of 30sec. All data were stored on the hard-disc, the readings of the remote unit were additionally

stored on the two 8 MB PCMCIA Flash memory cards. The system was checked on a daily basis by the remote connection via GSM modem and data of the last 24hours were downloaded.

5.4. Results & Discussion

5.5. Temperature and Gas Measurements June-October 2005

During the installation and monitoring period from June 8th to June 14th the condensation of water in the system has been never been observed, neither in the tubing nor in the built-in water-trap. As a water-trap causes a certain lag-time of the gas measurements (up to 10min, depending on the operating conditions) the water-trap was removed. However, after 7 weeks of continuous operation the measured values of the applied IR sensors became unstable (see below). Inspection of the sensors on October 17th revealed a condensation of water in the feed tubing's and the measuring cells. This can be caused by a simple condensation of water vapor in the system, because the night-time ambient and measuring box temperatures were usually 20 °C lower than day-time temperatures (not shown).

Another potential explanation is the fouling of the membrane (see Figure 27). Although the membrane has been successfully used in volcanic environments, a long-term application in combustion gas vents has never been tested before. The inspection of the membrane, after it had been installed for 5 months, revealed an intensive fouling with the high molecular weight hydrocarbons of the combustion gas. This might have degraded the dilution efficiency of the membrane ultimately resulting in a drastic increase of water vapor in the measuring gas.

Figure 27: Example of the original membrane as of June 14th and after removal at October 16th; the membrane is considerably fouled with condensates (disconnection between membrane and Teflon tubing occurred as a result of removal from the vent)

Due to a failure of the operating system of the controlling computer on August 25th (operating system hang-up during the re-boot sequence) the remote connection was lost and weather data have not been recorded until October 17th, 2005.

Temperature measurements show some remarkable fluctuations during relatively short time periods (Figure 28, Figure 29 and Figure 31). Short term temperature

variabilities are higher and more frequent at locations TL1.N-S and TL1.E-W than at the other locations.

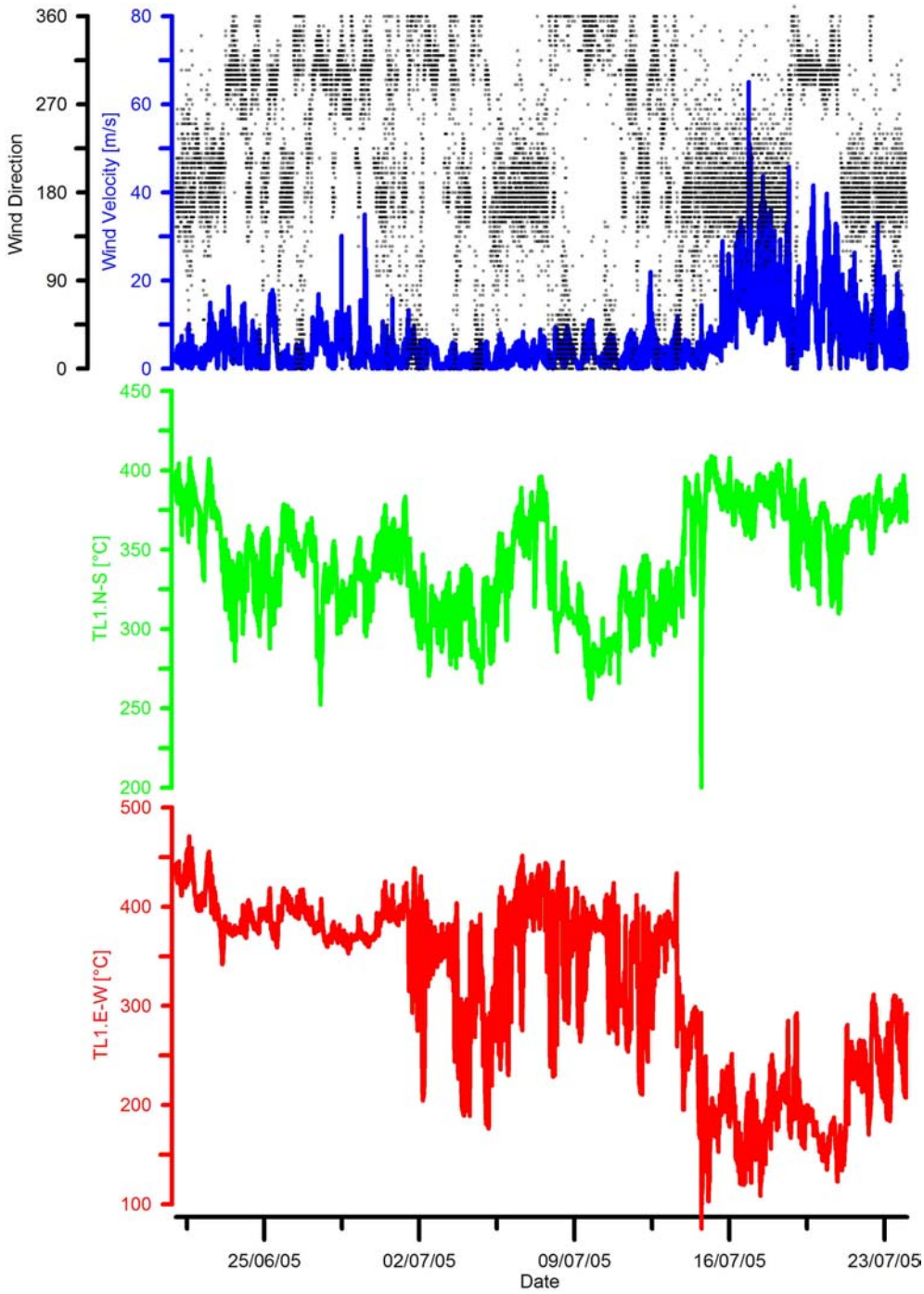

Figure 28: Temperature variances at location 1 from June 14th – July 24th 2005 and corresponding wind data (velocity and direction)

Temperature drops in excess of more than 200°C within one or two days have been observed at these two locations, though the temperatures raised likewise rapid to the previous levels. Temperature variations at location TL2 and TL3 were less pronounced but are still beyond the statistically significance level. However, it is evident, that the temperature variations at these locations are not only lower in terms of the absolute values - which could be expected - but also in terms of the relative changes. This might indicate that the vents with much higher temperatures are more affected by the

dynamic combustion process and turbulent gas flows than the lower temperature vents, where the flow regime is more stable due to the larger distance from the main zone of the combustion.

One typical illustration of the temperature variations is shown in Figure 28. At location TL1.E-W the temperature dropped in two phases. The first decrease of around 100°C (360°-> 260°) occurred during a time period of app. 7h on June 13th 13:15, the second step with a decline of 120°C (260°C -> 140°C) took place at June 14th 15:00 over a time period of approximately 6h. Within the same time period (June 14th,11:30) the temperature at location TL1.N-S increased by 60 °C (340°-> 400°C) within 10h. On the first glance it appeared that the temperature variations are related with the emerging gale force winds (wind speed higher than 40m/s, Figure 28). However, a detailed view of the data shows, that the weather conditions cannot be the reason for the observed temperature variations because the drastic change in wind conditions occurred not until June 15th 14:30.

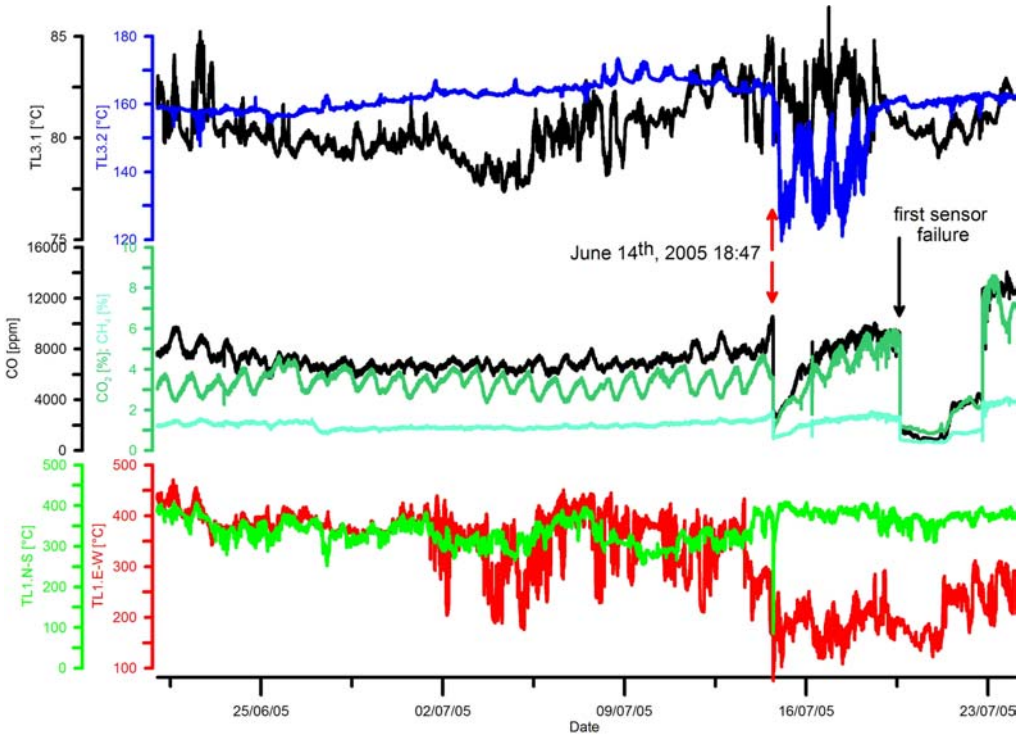

Figure 29: Gas composition and temperatures at location 3 and temperatures at location 1 (TL1.N-S, TL1.E-W) from June 21st to July 24th, 2005

At the same time (July 14th 18:47) similar changes in chemical composition of the combustion gases and of the temperature TL3.2 have been observed (Figure 29). TL3.2 dropped by roughly 40°C (165°C -> 125°C), the concentration of CO decreased by 70% (10000 ppm to 3000 ppm[4]), CO_2 by 60% (3.74% -> 1.4%) and CH_4 by 65% (1.8% -> 0.6%) within several minutes (see also Figure 30). Although there is also a simultaneous temperature drop at location TL3.1 at the same time, this is no proof for a correlation to the same external event, as this temperature change is not significantly different from other temperature variations occurring at this location.

[4] Concentrations have not been corrected for dilution (dilution factor about 5). Actual values are proxies only

It could be argued that the sharp decrease in gas concentrations is already the first indication of the sensor failures. However, two special features argue against this. The first one is the synchronous occurrence of other variations (e.g. temperature changes) on July 14th; the second one is the real-time history of the decrease. A detailed view of the relevant data from June 14th and June 19th clearly proves the difference. The sensor failure on July 19th is identified by an abrupt decrease, the timeframe only depending on the frequency of signal digitalization, whereas the unequivocal true effect on June 14th is identified by a continuous decrease over several minutes (Figure 30).

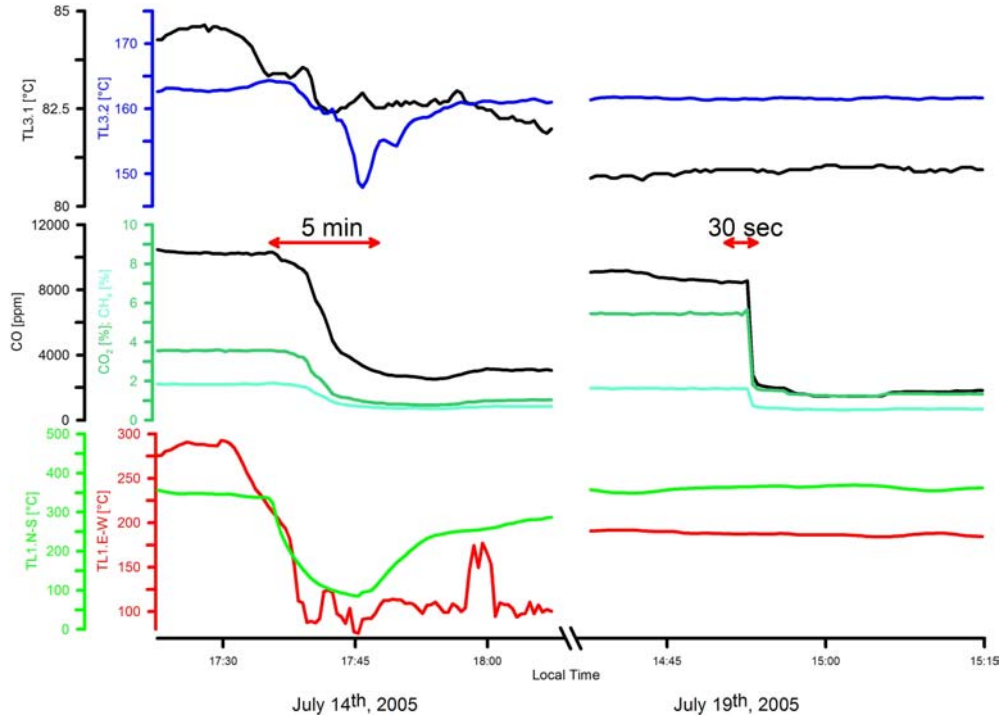

Figure 30: Detailed view of data (gas composition and temperatures) from July 14th and July 19th, illustrating two changes in gas composition at location 2

We have extensively analyzed the weather and temperature data, but we cannot establish a clear relationship between these two parameter sets (with the exception of location TL2.2, compare Figure 25). Occasionally it seems that the temperatures vary with wind direction (see for example Figure 34), at other times there is no correlation. Several reasons might account for this behavior (technical effects on temperature measurements can be excluded).

The simplest explanation would be the conclusion, that a 20m deep subsurface coal fire is simply representing a chaotic system which is not influenced by wind direction and velocity. However, we think that this conclusion is too simple-minded, because the special features of the coal fire under investigation (e.g. large collapse zone in the south with meter-wide deep fractures) let assume a certain causal relationship. It seems more possible, that the amount of local weather data is inadequate, due to the failure of the operation system after 10 weeks of continuous operation, to reveal the potential relations between combustion process (which is ultimately the reason for the observed temperatures) and external events like wind direction /velocity and barometric pressure.

The temperature variations could also originate from rain fall, as the fractures are open to the atmosphere. Although the regional climate is semiarid occasionally heavy rainfalls (e.g. thunderstorms) can occur. Unfortunately we do not have local or regional precipitation data to confirm or deny this hypothesis. The only data available are from Weather Online[5]. In Yinchuan (Ningxia Autonomous Region, about 100km south of Wuda) precipitation was reported from July 17th - July 21st and for Otog Qi (Inner Mongolia Autonomous Region, about 100km east of Wuda) from July 18th - July 21st.

Quite conceivable the response of the complex system "natural coal fire" on external weather influences is slow and potential effects may be masked by other factors. However, we think it is very important to obtain local, i.e. on-site, weather data, rather than meteorological observations from far-off weather stations (e.g. several kilometers) and to further investigate this correlation.

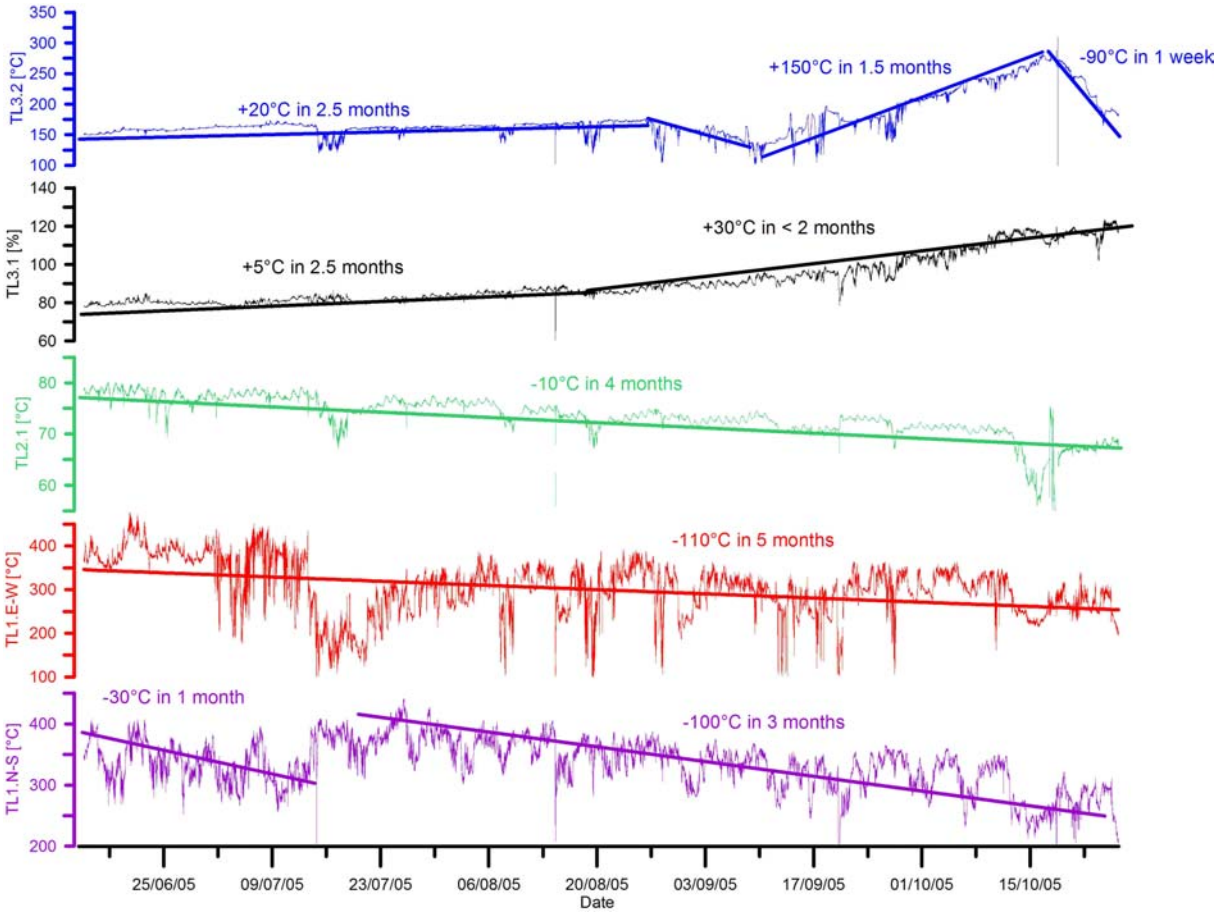

Figure 31: Observed long-term temperatures variances; numbers indicate the temperature decrease and increase of selected time intervals

Naturally there are other parameters influencing the combustion process and hence the measured temperatures. In particular unique events like collapsing roof walls can result in abrupt modification (e.g. jamming) of migration pathways for the combustion gases, hence disturbing the instable equilibrium between subsurface combustion and surface measurements. Normal fluctuation based on recurring changes in boundary

[5] http://www.weatheronline.co.uk/Asia.htm (last visited June 2006)

conditions (e.g. barometric pressure or other unidentified effects), can also be a reason for observed variations. However, a first FFT frequency and wavelet analysis of temperature data does not reveal a systematic short (i.e. daily or diurnal) or long-term oscillation. It is unlikely that other factors like changing chemical composition or humidity of the burning coal will be responsible for the observed short-term fluctuations.

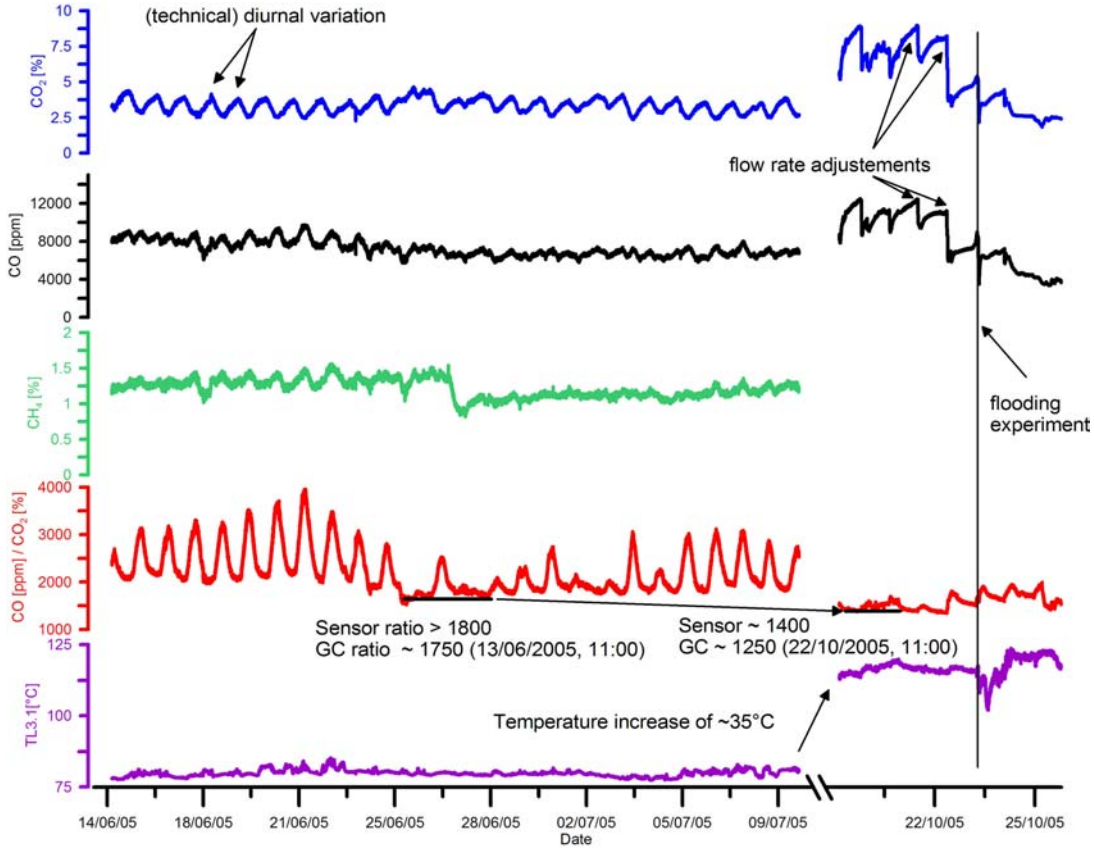

Figure 32: Long-term change in gas composition at location 2 (see text for explanation)

Besides the short-term variations we also find long-term trends which superimpose the temperature profiles (Figure 31). The temperatures at location TL1 generally decrease with time. TL1.N-S decreased by around 110° (from 350°C to 240°C) with an interim increase in mid July. The overall rate of temperature decrease is approximately -30°C/month. The trend for TL1.E-W is more speculative and obviously more disturbed by short-term fluctuations but still detectable, the temperature decrease amounts to 110°C in 5 months (rate app. -20°C/month).

Temperature decreases at location TL2.1 is less distinct but be clearly identifiable (-10°C in 5 months), despite the short-term variation during mid October.

Reverse trends are observed for gas temperatures at location 3. TL3.1 shows an overall temperature increase of 35°C (from 80°C to 115°) occurring with two different rates (Figure 31). At location TL3.2 a more complex development is observed. The temperature increases, beginning with a smooth temperature increase during the first 10 weeks (-20°C), interrupted by a momentary decline and a very a sharp increase from mid September until mid October (+150°C in approximately 6 weeks) followed by a very sharp decline during the last two weeks of the measuring period (-90°C in 1 week). Most likely the observed temperature trends are a result of the slowly

advancing fire front. The front moves in a north-easterly rather than a northerly direction as evidenced by the temperature trend at location TL3.2 in the southwest, temperature increase in the northeast (TL3.1) combined with a slight decrease at location 2. As the temperature changes are moderately we conclude that the fire propagation is relatively slow in this area, much slower than the occasionally supposed rates in excess of 50m/year.

Consistent with this assumption are also the results of the gas composition measurements. Upon arrival at the measuring site on October 16th, we replaced the defective CO and CO_2 IR sensors and the primary membrane in the vent at location TL3.1. Subsequently we continuously measured the composition of the emanating gases until October 26th for correlation with the DMT flooding experiments (see below).

Figure 32 shows the long-term variations of the combustion gases for two time intervals. The sinusoidal variations in the concentrations are a technical artifact (concentration varies with the strong ambient temperature undulation during summer time). In particular it was not possible to protect the CO_2 sensor from the massive temperature changes in the remote measuring unit. Therefore also the ratio CO/CO_2 (ppm/%) varies strongly with a diurnal frequency. These fluctuations vanished in October when the differences in day and night temperatures were much smaller (Figure 32).

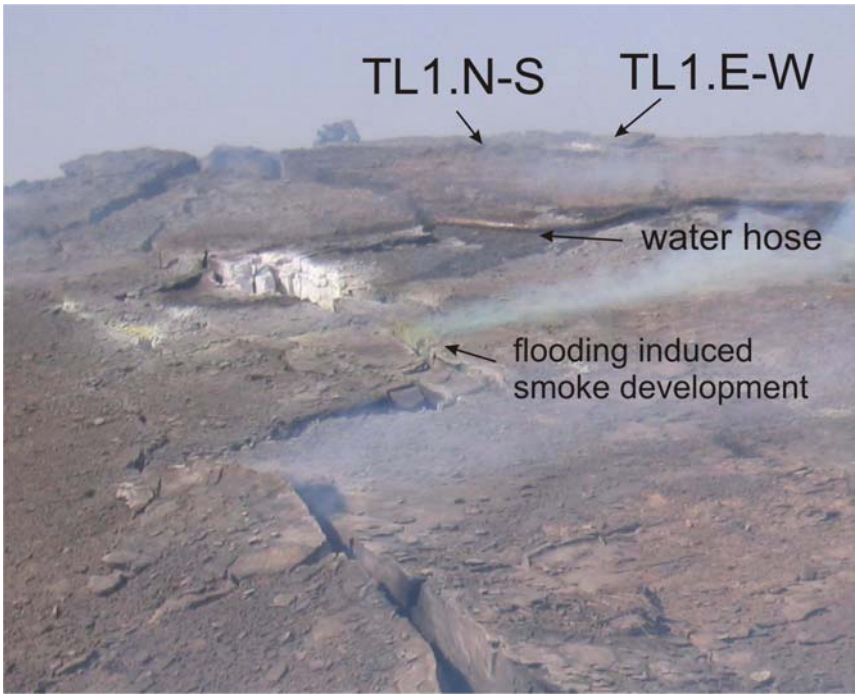

Figure 33: 1st flooding test (October 23rd, about 4.5m³ of water introduced) at location 1, see Figure 23 for detailed view of thermocouple positions

The major finding of the gas monitoring is the reduction of the CO/CO_2 ratio between June and October 2005. During June and July the ratio typically amounted for values between 1800 and 1900 (determined at the low points of the concentration profile). The determined ratio in the second half of October was significantly lower, around

1400. These results were further confirmed by GC measurements of gas samples in our laboratory, one sample taken on July 13th, the second on October 22nd (see Figure 32). This change in chemical composition further supports the explanation of the advancing fire front, as the fraction of combustion gases will increase (compared to products of the gasification process), hence more CO_2 will be generated compared to CO.

5.6. Effect of flooding experiments

During the October field work DMT performed several flooding test in order to induce microcracks close to the installed micro-acoustic monitoring station. The overall objective was to verify that crack developing can be measured and quantified (in terms of location and orientation). The three experiments were performed at several locations with different amounts of water.

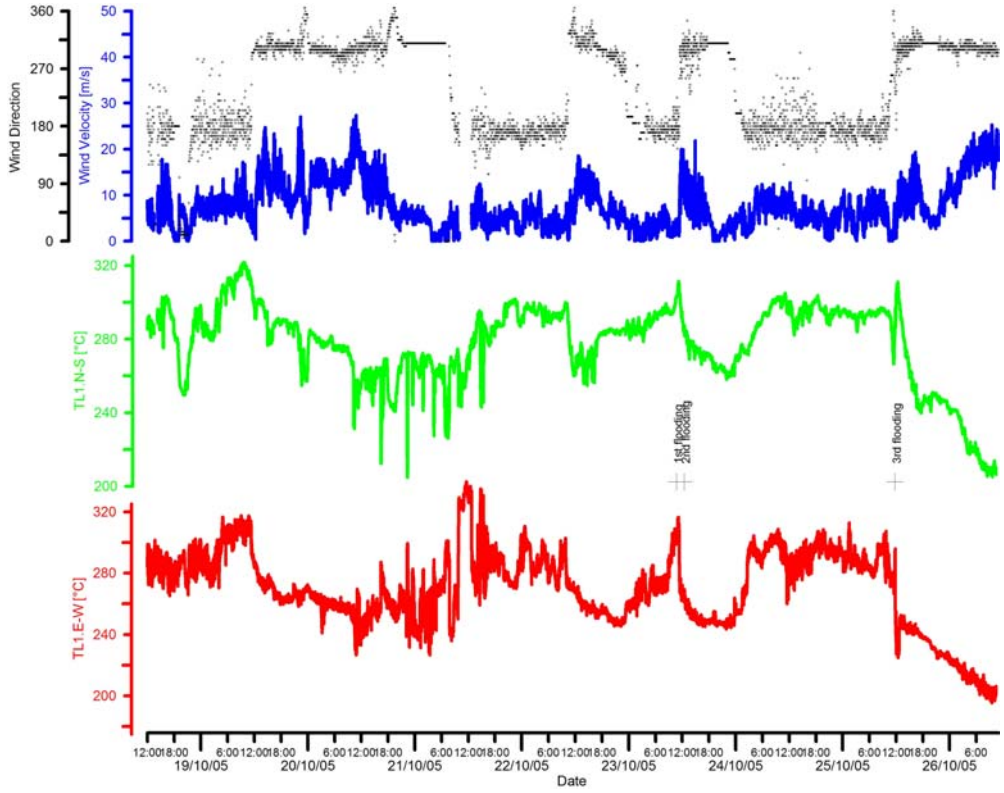

Figure 34: Temperature (location 1) and wind data for October 18th to October 26th

The first experiment was carried out close to the location 1. 4.5 m³ of fresh water were discharged from a truck into a large crack 5m downhill of the installed thermocouples TL1.N-S and TL1.E-W (Figure 33) through a fire fighting hose. The water flow lasted for approximately 75 minutes (10:30 – 11:45 local time). Temperature profiles of TL1.N-S and TL1.E-W are shown in Figure 34 and Figure 35. The temperature TL1.N-S dropped from 310°C -> 270°C with a smooth decline over two hours, whereas TL1.E-W showed a sharp temperature decrease by about 50°C during 10 minutes. However, these temperature variations coincide with a significant change in wind direction (from S to W) and wind velocity (2m/s -> up to 15m/s, Figure 35) and it cannot be ruled out, that the observed variations are a result of the external weather conditions rather than of the water flooding. This latter explanation is further supported

by the observation, that only downhill of the water injection place steam emissions were observed, but no visible effects in fractures uphill.

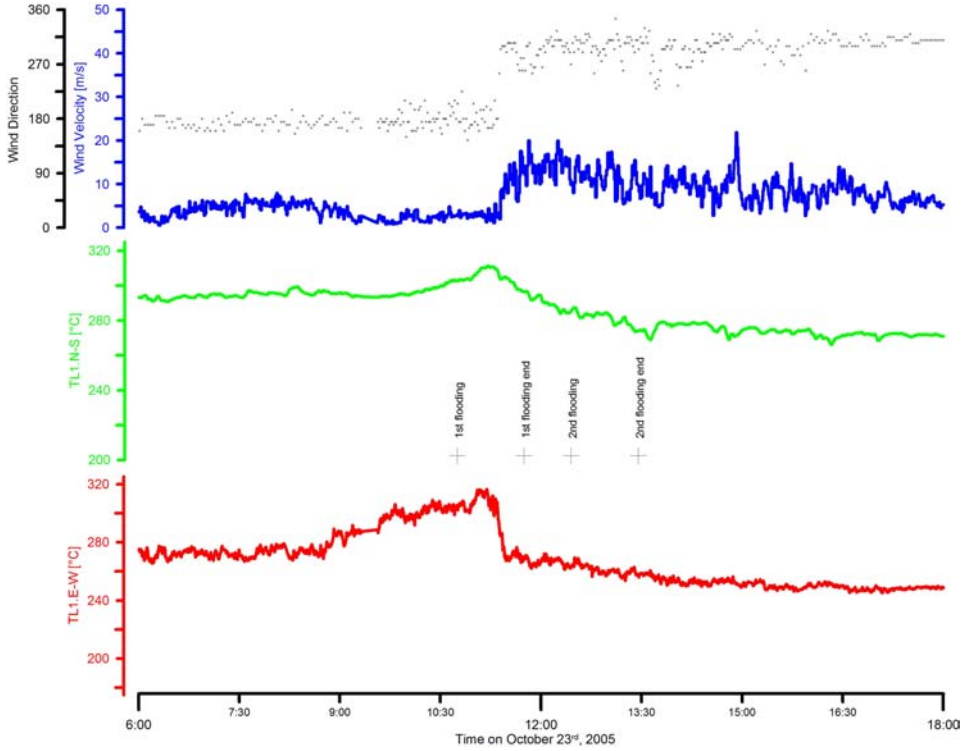

Figure 35: Detailed view of temperature profiles during flooding experiments 1 and 2

The second flooding experiment was performed close to our measuring location 3. Approximately 3m west of this location another 4.5m³ of water were flown into a small fracture which appears to be an extension of the main E-W rupture zone (see Figure 26 and Figure 36). Shortly after the start of the flooding (after about 5minutes), a strong steam emission at location TL3.1 was observed (Figure 37). This had a strong effect on the measured gas composition (Figure 38), both CO and CO_2 concentration decrease sharply due to the dilution effect of steam but the CO_2/CO ratio did not change (not shown).

The effect of the temperatures at the three different measuring points is complex. Corresponding to the change in gas composition the temperature at location TL3.1 decreased sharply (from 117°C -> 109°C), increased again for a few minutes and was than followed by a constant decline until the end of the flooding experiment. The temperature drop at TL3.1 around 10:30 is most likely an effect of the changing wind conditions and not a result of the flooding experiment 1 as the distance is too far. The response of the more distant TL3.2 temperature measurement (about 2m to the east in the same fracture) was delayed by around 25min from the start of experiment.

Figure 36: October 23rd: 2nd flooding test (about 4.5m³ water flooding close to the monitoring location 3)

Figure 37: Steam eruption at location TL3.1, shortly after flooding experiment started

Similar to TL3.1 the temperature increased shortly (< 5°C) and than showed a smooth and constant decline from ~215°C down to 195°C. Amazingly, the temperature at the recently installed location TL3.3 almost immediately decreases after the start of the experiment, despite the fact, that this location is the most distant from the point of water injection (about 5m, Figure 26). In summary, the effects of the water flooding on

the measured temperatures were relatively small, much lower than we expected (10°-15°C) and are unlikely a result of the changing wind conditions (unless there would be a lag time of at least two hours between wind change and temperature response).

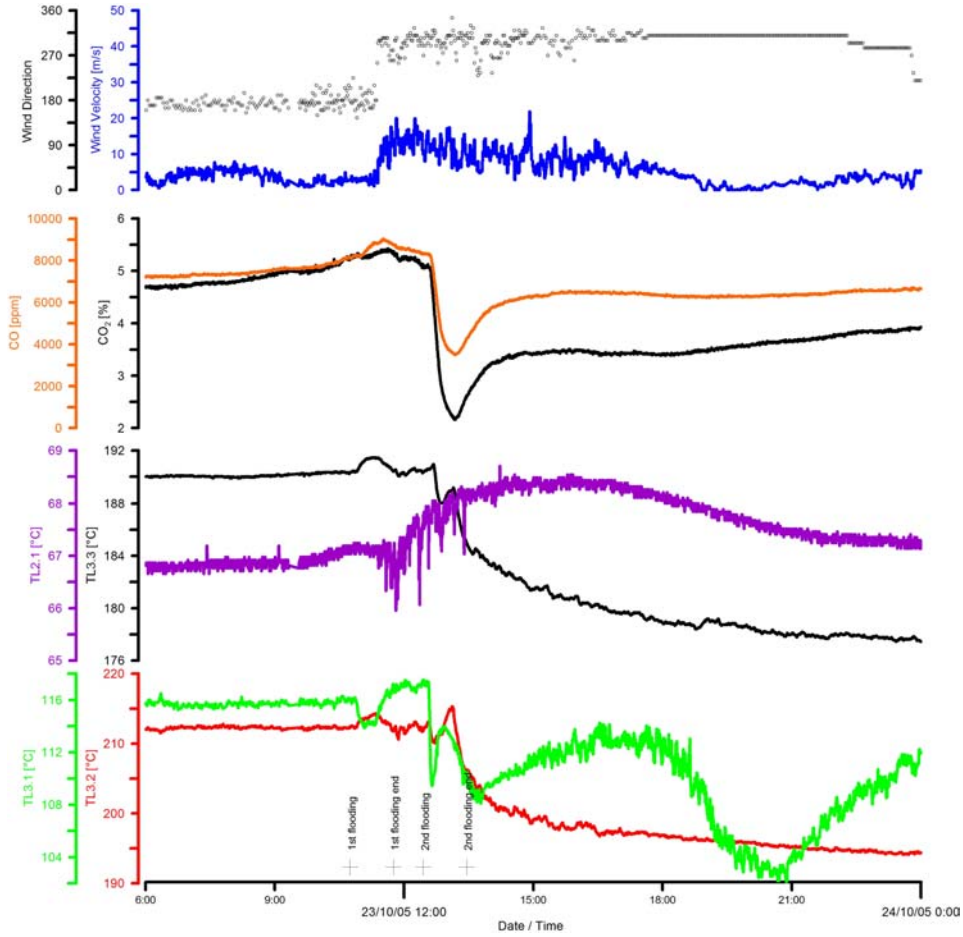

Figure 38: Gas composition and temperature variations as a function of the flooding experiment near monitoring location 3

The third flooding experiment was performed close to injection location 1. Around 15m³ of water were delivered by two trucks and subsequently simultaneously flowed into a large fracture (0.5m width, Figure 23) close to the main combustion zone where red-hot bedrock can be observed (not shown). Shortly after the experiment started heavy steam burst out could be observed. The temperature record of TL1.N-S shows a two-phase development, where the first one, a decline from 295°C -> 260°C, occurs before the water flooding started (Figure 39). This decline is followed by sharp increase of the temperature. Both developments could be a result of wind changes which occur contemporaneously (Figure 39). The second and ultimate drop in the temperature at location TL1.N-S occurs shortly after the flooding experiment started and the steam eruption was observed. The temperature decline has an exponential form until 6 hours after the water injection stopped. Afterwards the temperature continues to drop almost linearly for the next 15hours when the thermocouple had to be removed. The temperature at TL1.E-W shoes a more or less vertical drop by 50°C (from 270°C -> 220°C), followed by a short and less significant temperature increase. One hour after stopping the water injection the temperature starts decreasing almost linearly (Figure 39). Even though the measuring period and the obtained data after the

third experiment are only very limited (due to the de-installation), we conclude that the third flooding experiment had a strong effect on the combustion processes in this part of the coal fire. Presumably the combustion ceased and the temperature decline is reflecting the cooling of the overlying rocks.

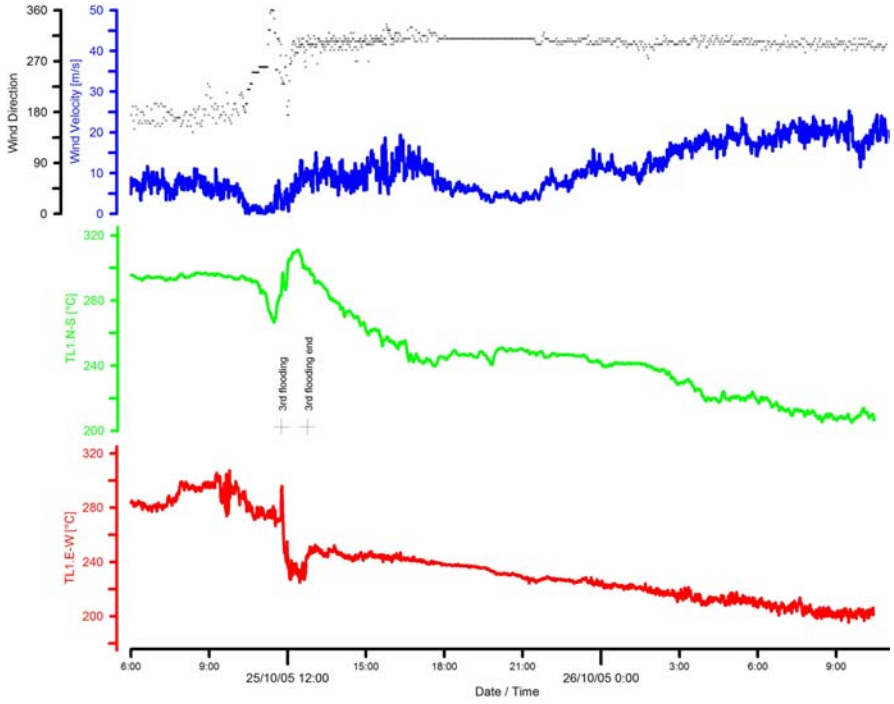

Figure 39: Temperature profile of TL1.N-S and TL1.E-W after flooding experiment 3

5.7. Summary Permanent Monitoring 2005

The analysis of combustion gases is of major importance for the understanding of natural coal fire combustion processes, which in turn is important for all corrective measures (fire fighting and fire preventing). Gas measurements are essentially the sole and exclusive way to analyze the combustion process in the subsurface. In addition these data are used to set-up and validate static and dynamic 3-D models of the in-situ coal combustion process. By means of gas measurements active fire and ventilation zones can be detected in an early stage.

In 2004 extensive investigations of the combustion gases have been carried out at two selected fire zones (8 and 3.2) of the Wuda Coal Mining Area (Inner Mongolia Autonomous Region, PRC) within the framework of the "Sino-German Coal Fire Research Project". These investigations comprised measurements of CO_2, CO, H_2S, O_2 and CH_4 by means of a multigas-sensor device (Multiwarn II) accompanied by temperature measurements of the vents. Based on the results a site for permanent long-term gas and temperature monitoring station was selected. Long-term monitoring of gas emanations from July to October 2005 resulted in high data density of combustion products (minute scale), temperature of gases, and weather conditions parameters (air pressure, temperature, wind direction and velocity) revealing the temporal and long-term changes in the dynamics of the combustion process.

The results from combustion gas measurements clearly revealed that natural coal fires are very complex system. Based on the chemical composition of the vent gases it became evident that one fire zone compared to another can be completely different, e.g. FZ 8 and 3.2 are clearly distinguishable by their methane content in the

combustion gases. This evidently follows the different general set-up of fire zones, like actual combustion process, geological situation, depth and existing crack system, etc. However, also on a smaller scale, i.e. within fire zones, coal fires are very inhomogeneous in terms of temperature distribution and gas composition. Non-combustion products like hydrocarbons (methane and higher homologues) and molecular hydrogen were detected in significant amounts (up to 9% CH_4 and 3.2% H_2) at fire zone 8. This shows that different combustion processes (pyrolysis and coking /gasification) occur concurrently in very small zones, but the overall contribution of a single process is hardly to be resolved. Therefore no unique relationship between gas composition, gas ratios and temperature could be established. This is most likely due to the very complex system of vents and fire induced large cracks. The measured gases are possibly a mixture of the combustion gases from different locations, partly diluted by air, which are merging together and emanating from single fractures.

The site for the permanent monitoring was selected on the base of the previous results. For the gas measurements we have chosen a location where relatively low temperatures (<100°C) prevailed and higher-than-average amounts of non-combustion products (H_2, CO, CH_4) were detected in the emanating gases. At this site we expected the best opportunity to perceive the approaching fire front. At two additional sites temperature measurements were performed and meteorological data were recorded. The data from the long-term surveillance of fire zone 8 showed that the temperatures of gas emanating vents are highly variable in terms of short-range fluctuations, which also holds for the chemical composition of the gases. The interrelation of these variations with the prevailing meteorological conditions (barometric pressure, wind direction and velocity) is very complex and still unresolved. The dynamics of the subsurface coal fire are only observable by long-term measurements. Different rates of temperature decrease/increase at discrete locations and a change of the diagnostic CO/CO_2 ratio indicate a slow (< 10m/year) advancing fire front in a north-easterly direction.

For a follow-up project (application pending) it is intended to operate continuously a similar but more simplified monitoring station to determine a base line of gas emissions, keep the corrective measures (i.e. fire extinction process) under observation and apply this kind of monitoring for a long-term, permanent and self-acting surveillance of extinguished fire zones. Main objective is an early warning in case of re-ignition of the subsurface coal combustion.

References

Álvarez, R., Clemente, C. & Gómez-Limón, D., 1997. Reduction of thermal coals, environmental impact by nitric precombustion desulfurization. *Environmental Science and Technology* 31(11): 3148-3153.

Barysheva, L.V., Borisova, E.S., Khanaev, V.M., Kuzmin, V.A., Zolotarskii I.A., Pakhomov, N.A. & Noskov, A.S., 2003. Motion of particles through the fixed bed in a gas-solid-solid downflow reactor. *Chemical Engineering Journal*, 91(2): 219-225.

Brasseur, A., Antenucci, D., Bouquegneau, J.M., Coëme, A., Dauby, P., Létolle, R., Mostade, M., Pirlot, P. & Pirard, J.-P., 2002. Carbon stable isotope analysis as a tool for tracing temperature during the El Tremedal underground coal gasification at great depth. *Fuel*, 81(1): 109-117.

Bräuer, K., Kämpf, H., Faber, E., Koch, U., Nitzsche, H., & Strauch, G., 2004. Gas and carbon isotope composition of methane: monitoring results in relation to the Vogtland-NW Bohemia earthquake swarm period 2000. *Geochemical Journal* (subm.)

Brune, S., Faber, E., Teschner, M., Poggenburg, J. & Hagendorf, J., 2003. CO_2-deposits at Vorderrhön area (Thuringia) – Gas migration from a deep reservoir to surface ? International Conference on Gas Geochemistry – ICGG7, Freiberg/Germany, September 22nd-29th.

Busch, A., Krooss, B. M., Gensterblum, Y., van Bergen, F. & Pagnier, H. J. M. (2003): High-pressure adsorption of methane, carbon dioxide and their mixtures on coals with a special focus on the preferential sorption behaviour. - Journal of Geochemical Explora-tion, 78-79, 671-674

Bergfeld, D., Goff, F. & Janik, C. J. (2001): Elevated carbon dioxide flux at the Dixie Valley geothermal field, Nevada; relations between surface phenomena and the geothermal reservoir. *Chemical Geology* 177: 43-66.

Cardellini, C., Chiodini, G., Frondini, F., Granieri, D., Lewicki, J. & Peruzzi, L. (2003): Accumulation chamber measurements of methane fluxes: application to volcanic-geothermal areas and landfills. *Applied Geochemistry*: 18, 45-54

Chamberlain, E.A.C., 1979. The ambient temperature oxidation of coal. – National Coal Board, Hobart House, London

Chandelle, V., Jacquemin, C., Létolle, R., Mostade, M., Pirard J.-P. & Somers, Y., 1993. Underground coal gasification on the Thulin site: results of analysis from post-burn drillings. *Fuel* 72(7): 949-963.

Conti, R.S. & Litton, C.D., 1995. A Comparison of Mine Fire Sensors. NIOSH Report of Investigations 9572

Cosca, M.A., Essene, E.J., Geissman, J.W., Simmons, W.B., & Coates, D.A., 1989. Pyrometamorphic rocks associated with naturally burned coal seams, Powder River Basin, Wyoming. *American Mineralogist* 74: 85– 100.

Creedy, D.P., Garner, K., Holloway, S., Jones, N. & Ren, T.X., 2001. Review of Underground coal gasification technological advancements. *DTI/Pub URN 01/1041*, Report No. COAL R211

Dalverny, L.E. & Chaiken, R.F., 1991. Mine fire diagnostics and implementation of water injection with fume exhaustion at Renton, PA. – US Bureau of Mines RI 9363, 42pp.

de Jong, W., Unal, O., Andries, J., Hein, K.R.G. & Spliethoff, H., 2003. Thermochemical conversion of brown coal and biomass in a pressurised fluidised bed gasifier with hot gas filtration using ceramic channel filters: measurements and gasifier modelling. *Applied Energy* 74(3): 425-437.

de Rosa, M., 2004. Analysis of Mine Fires for All U.S. Underground and Surface Coal Mining Categories: 1990-1999. *NIOSH Publication No. 2004-167*, U.S. Department of Health and Human Services, Centers for Disease Control and Prevention, National Institute for Occupational Safety and Health

Delisle, G.; Teschner, M.; Panahi, B.; Iguliev, I.; Aliev, Ch. & Faber, E., 2005. Continuous one year record of methane flux from the Dashgil mud volcano/Azerbaijan. General Assembly European Geosciences Union, Vienna/Austria, April 24th-25th

Diaz, C.M., Wagner, R.H., Winkler, Prins, C.F & Granados, L.F., 1983. The Carboniferous of the World. Vol. China, Korea, Japan and S. E. Asia. *IUGS Publications N° 16*; Available only through Comercial General Del Libro y Material Didactico, S.A., C/Reina No. 15, 28004 Madrid, Spain. 11-177

Dickeç, F., Ateşok, G. & Arslan, C., 1994. Coking of Coal. – in: Kural, O. (ed.) *Coal*. – Istanbul Technical University, Istanbul, Turkey, 309-335

DOE 1993. The Fire Below: Spontaneous Combustion in Coal. *Environmental Safety and Health Bulletin*, EH-93-4, Issue No. 93-4, US Department of Energy

Edwards, J.C., Franks, R.A., Friel, G.F., Lazzara, C.P. & Opferman, J.J. 1999. Mine Fire Detection in the Presence of Diesel Emissions. In: Thien, J.C. (ed.), *Proceeding of the Eighth U.S. Mine Ventilation Symposium*. Rolla, MO: University of Missouri-Rolla, Press, 295-301

Faber, E., Móran, C., Poggenburg, J., Gárzon, G., Teschner, M., 2003. Continuous gas monitoring at Galeras volcano, Columbia: first evidence. *Journal of Volcanology and Geothermal Research* 125:13-23.

Feng, J., Li, W.-Y. & Xie, K.-C. 2004. Relation between coal pyrolysis and corresponding coal char gasification in CO_2. *Energy Sources* 26: 841-848.

Gangopadhyay, P.K., 2003. Coalfire detection and monitoring in Wuda, North China: A Multi-spectral and Multi-sensor TIR Approach. Master's thesis. Enschede, The Netherlands: International Institute for Geo-Information Science and Earth Observation (ITC).

Gielisch, H. & Kahlen, E., 2003. Innovative Technologies for Exploration, Extinction and Monitoring of Coal Fires in North China: Work Package 2210, Geology of the Helan Shan. Unpublished Project Report. Essen, Germany: Deutsche Montan Technologie GmbH

Gönenç Sunol, Z.S. & Sunol, A.K., 1994. Pyrolysis of coal. – in: Kural, O. (ed.) *Coal*. – Istanbul Technical University, Istanbul, Turkey, 338-351

Graham, J.I., 1920. The normal production of carbon monoxide in coal mines. – *Transactions of the Institution of Mining Engineers* 60: 222-231.

Grosshandler, W.L., 1995. A Review of Measurements and Candidate Signatures for Early Fire Detection. National Institute of Standards and Technology, Building and Fire Research Laboratory, NISTIR5555 Gaithersburg, MD 20899

Harju, J.B., 1980. Coal Combustion Chemistry. *Pollution Engineering*, May 1980, 54-60.

Harris, D.J., Roberts, D.G. & Henderson, D.G., 2006. Gasification behaviour of Australian coals at high temperature pressure. *Fuel* 85: 131-142.

Heffern, E.L. & Coates, D.A., 2004. Geologic history of natural coal-bed fires, Powder River basin, USA. *International Journal of Coal Geology* 59: 25-47.

Herman, A. and McAteer, J.D., 1999. Estimating the Rate of Coal Combustion in a Mine Fire. U.S. Department of Labor, Mine Safety and Health Administration, IR 1249

Huang, L., Bruining, J. & Wolf, K.-H.A.A., 2001. Modelling of gas flow and temperature fields in underground coal fires. *Fire Safety Journal*, 36: 477-489.

Hunt, J.M., 1996. Petroleum Geochemistry and Geology. – Freeman, New York, 743pp.

Jones, J.H. & Trickett, J.C., 1955. Some Observations on the examination of gases resulting from explosions in colleries. *Transactions of the Institution of Mining Engineers* 44: 768-791.

Jones, P.J., 1995. *Carboniferous*. Timescales 5. Australian. Geological Survey Organisation, Record 1995/34

Jones, V.T., & Thune, H.W., 1982. Surface detection of retort gases from an underground coal gasification reactor in steeply dipping beds near Rawlins, Wyoming. *Society of Petroleum Engineers*, SPE 10050.

Kim, A.G. & Chaiken, R.F., 1993. Fires in Abandoned Coal Mines and Waste Banks. – United States Department of the Interior, Information Circular 9352.

Kim, A.G., 1986. Signature criteria for monitoring abandoned mine fires. – Proceedings of the 8th Annual National Abandoned Mined Lands Conference, Billings, Montana.

Kim, A.G., 1991. Laboratory determination of signature criteria for locating and monitroing abandoned mined land fires. – Bureau of Mines RI 9348.

Klika, Z., Kozubek, T. Martinec, P. Klikova, C. & Dostal, Z., 2004. Mathematical modeling of bituminous coal seams burning contempraneously with the formation of variegated beds body. *International Journal of Coal Geology* 59: 137-151.

Kroonenberg, S.B. & Zhang, X., 1997. Pleistocene coal fires in north-western China, Energy for early man. In van Hinte, J.E. (ed.) *One Million Years of Anthopogenic Global Environmental Change*. Proceedings of the ARA Symposium at the Royal Netherlands Academy of Art and Sciences (KNAW), Amsterdam, Project ID 2-74690, 39-44.

Krooss, B.M., van Bergen, F., Gensterblum, Y., Siemons, N., Pagnier, H.J.M. & David, P., 2002. High-pressure methane and carbon dioxide adsorption on dry and moisture-equilibrated Pennsylvanian coals. *International Journal of Coal Geology* 51: 69-92.

Kwiecińska, B., Hamburg, G. & Vleeskens, J., 1992. Formation temperatures of natural coke in the Lower Silesian Coal Basin, Poland. Evidence from pyrite and clays by SEM–EDX. *International Journal of Coal Geology* 21: 217–235.

Kwiecińska, B., Muszynski, M., Vleeskens, J. & Hamburg, G., 1995. Natural coke from the La Rasa mine, Tineo, Spain. *Polskie Towarzystwo Mineralogiczne* 26: 3 – 14.

Kwiecińska, B. & Petersen H.I., 2004. Graphite, semi-graphite, natural coke, and natural char classification—ICCP system. *International Journal of Coal Geology* 57: 99-116.

Kuyper, R.A., van der Meer, Th.H. & Bruining, J., 1996. Simulation of Underground Gasification of Thin Coal Seams. *In Situ*, 20(3): 311-346.

Li, C.-T., Mi, H.-H., Lee, W.-Y., You, W.-C. & Wang, Y.- F., 1999. PAH emission from the industrial boilers. *Journal of Hazardous Materials* 69(1): 1-11.

Litschke, T., Wiegand, J., Schlömer, S., Gielisch, H. & Bandelow, F.-K. (submitted): Detailed mapping of coal fire sites in combination with in-situ flux measurements of combustion-gases to estimate gas flow balance and fire development (Wuda coal field, Inner Mongolia, PR China). – submitted to ERSEC Ecological Book Series, Volume4

Ökten, G. & Didari, V., 1994. Underground Gasification of Coal. – in: Kural, O. (ed.) *Coal*. – Istanbul Technical University, Istanbul, Turkey, 371-378.

Megaritis, A., Messenböck, R. C., Collot, A.-G., Zhuo, Y., Dugwell, D.R. & Kandiyoti, R., 1998. Internal consistency of coal gasification reactivities determined in bench-scale reactors: effect of pyrolysis conditions on char reactivities under high pressure CO_2. *Fuel* 77(13): 1411-1420.

Minchener, A.J., 2005. Coal gasification for advanced power generation. *Fuel* 84: 2222-2235.

Mitchell, D.W., 1996. *Mine Fires, Prevention-Detection-Fighting*. Intertec Publishing, Chicago

Moreea – Taha, R., 2000. *Modelling and simulation for coal gasification*. IEA Coal Research

Onozaki, M., Watanabe, K., Hashimoto, T., Saegusa H. & Katayama, Y., 2006. Hydrogen production by the partial oxidation and steam reforming of tar from hot coke oven gas. *Fuel* 85(2): 143-149.

Parker, L.W., Miller, J., Steinberger, Y. & Whitford, W.G.(1983): Soil respiration in a chihuahuan desert rangeland. - Soil Biology and Biochemistry, 15/3, 303-309

Perkins, G., 2004. Coupling dominant surface submodels and compley physical process Computational Fluid Dynamics. *Australian and New Zealand Industrial and Applied Mathematical Journal* 45: C817-C830.

Poggenburg, J., & Faber, E., 2004. Offenlegungsschrift DE 10240330A1, *Deutsches Patent- und Markenamt München.*

Prakash A. & Gupta, R.P., 1999. Surface fires in Jharia coalfield, India - their distribution and estimation of area and temperature from TM data. *International Journal of Remote Sensing 20*, 1935-1946.

Schloemer, S., 2005. Innovative Technologies for Exploration, Extinction and Monitoring of Coal Fires in North China: Intermediate Report Intermediate Report WP 3410 & 3420 (Gas Geochemistry of Combustion Gases), Unpublished Project Report. Bundesanstalt für Geowissenschaften und Rohstoffe (Hannover, Germany).

Schobert, H.H. & Song, C., 2002. Chemicals and materials from coal in the 21st century. *Fuel* 81: 15-32.

Schobert, H.H., 1987. *Coal - The Energy Source of the Past and the Future*. – American Chemical Society, Washington DC, USA, TP325 S34

Seidl, D., Hellweg, M., Calvache, M., Gomez, D., Ortega, A., Torres, R., Böker, F., Buttkus, B., Faber, E., & Greinwald, S., 2003. The multiparameter station at Galeras Volcano (Colombia) - concept and realization. *Journal of Volcanology and Geothermal Research* 125: 1-12.

Sekine, Y., Ishikawa, K., Kikuchi, E., Matsukata, M & Akimoto, A., 2006. Reactivity and structural change of coal char during steam gasification. *Fuel* 85: 122-126.

Stillman, R., 1979. Simulating of a Moving Bed Gasifier for a Western Coal. *IBM Journal of Research and Development* 23(3): 240-250.

Stracher, G.B., 2004. Coal fires burning around the world: a Global Catastrophe. – *International Journal of Coal Geology* 59: 1-6.

Stracher, G.B. 2003. Coal Mine Fire – Gas and Condensation Products: Collection Techniques for Laboratory Analysis. *Energeia* 14(5): 1-6.

Stracher, G.B., 1995. The anthracite smokers of eastern Pennsylvania: $P_{S_{2(g)}}$ stability diagram by TL Analysis. *Mathematical Geology* 27(4): 499-511.

Stracher, G.B. & Taylor, T.P., 2004. Coal fires burning out of control around the world: thermodynamic recipe for environmental catastrophe. *International Journal of Coal Geology* 59: 7-17.

Taylor, G.H., Teichmüller, M., Davis, A., Diessel, C.F.K., Littke, R. & Robert, P., 1998. *Organic Petrology*. Gebrüder Borntraeger, Berlin-Stuttgart. 704 pp.

Teschner, M., Vougioukalakis, G.E., Faber, E., Poggenburg & J., Hatziyannis, G., 2005. Real time monitoring of gas-geochemical parameters in Nisyros fumaroles. In: Fytikas, M. & Vougioukalakis, G. (eds.) *The South Aegean Volcanic Arc: Present Knowledge and Future Perspectives,* Proceedings for the International Meeting, Milos/Greece, September 17th -20th, Elsevier

Teschner, M., Faber, E., Poggenburg, J., Vougioukalakis, G.E. & Hatziyannis, G., 2006. Real-time gas-geochemical surveillance on Nisyros island (Aegean Sea, Greece) – Installation and continuous operation of a direct monitoring system in hydrothermal vents. – Submitted to Pure and Applied Geophysics (PAGEOPH)

Thompson, H., 1999. Comparison of predicted equilibrium nitrogen-, oxygen- and sulphur-containing organic species concentrations in coke oven emissions and gases with observations . *Fuel Processing Technology*, 61(3): 243-263.

Tissot, B.P. & Welte, D.H., 1984. *Petroleum formation and occurence*. Springer, Berlin-Heidelberg-New York-Tokyo, 699 pp.

Thunman, H. & Leckner, B., 2003. Co-current and counter-current fixed bed combustion of biofuel-a comparison. *Fuel*, 82(3): 275-283.

Ünal, S., Piskin, S. & Williams, A. 1994. Coal Gasification. – in: Kural, O. (ed.) *Coal*. – Istanbul Technical University, Istanbul, Turkey, 353-370.

Wall, T.F., Liu, G.-S., Wu, H.-W., Roberts, D.G., Benfell, K.E., Gupta, S., Lucas, J.A. & Harris, D.J., 2002. The effects of pressure on coal reactions during pulverised coal combustion and gasification. *Progress in Energy and Combustion Science* 28(5): 405-433.

Welles, J. M., T. H. Demetriades-Shah, & McDermitt, D. H. (2001): Considerations for measuring ground CO2 effluxes with chambers. *Chemical Geology* 177, 3-13

Yang, L., 2004. Study on the model experiment and numerical simulation for underground coal gasification. *Fuel* 83: 573-584.

Yang, L., Jie, L.,& Li Y., 2003. Clean coal technology — Study on the pilot project experiment of underground coal gasification. *Energy* 28(14): 1445-1460.

Zhang,X. & Kroonenberg, S.B., 1996. Pleistocene coal fires in Xinjiang, northwest China. – Abstracts of the 30th International Geologic Congress, Beijing, China (August 4th-14th) 1, 457

Zhuo, Y., Herd, A.A. & Kandiyoti, R., 2003. Thermochemical reactions of middle rank coals. In Ikan, R. (ed.) *Natural and Laboratory-Simulated Thermal Geochemical Processes*, Kluewer Academic Publishers, 53-152